Climate Dynamics (2026) 64:113
https://doi.org/10.1007/s00382-026-08061-y

ORIGINAL ARTICLE

Drivers of evapotranspiration in Central Africa: investigating seasonality and change in interactions with soil moisture, and solar radiation

Stella Songwe Tikeng[1] · Wilfried Mba Pokam[1,2] · Ellen Dyer[3] · Rachel James[4]

Received: 2 April 2025 / Accepted: 8 January 2026

Abstract

The present study uses 41 years of ERA5 and MERRA2 reanalysis data to assess Soil moisture-Evapotranspiration Interactions (SEIs) and the contribution of surface solar radiation (SSR) to evapotranspiration (ET) variability in Central Africa (CA). The study area is clustered using the k-means method, and the nature and strength of changes in ET induced by soil moisture (SM) and SSR are assessed. A comparative evaluation of the performance of MERRA2 and ERA5 in representing SEIs is also made. The results indicate that transitional areas (wet and dry areas) show a strong significant control of SM on ET, while very wet areas show a weak but almost significant sensitivity of ET to changes in both SM and SSR. MERRA2 shows an extreme sensitivity of ET to changes in SM, resulting in a failure to capture the competitive controls on ET exerted by surface versus root zone SM during wet and dry seasons, particularly in dry and very dry soil regimes. The two reanalysis datasets reveal a possible interaction between SM and SSR in very wet area, which could impact SEIs. A rapid drying process, accompanied by a hydrometeorological regime transition, may be currently underway in the CA region. The most significant and strongest transition seems to be occurring in very wet area. The seasonal meridional migration of the strong response of ET to changes in SM is associated with a switch in the control of ET between SM and SSR. The switch in control depends on soil water content, cloud cover and land cover. When considering the surface versus the root zone soil layer, a shared control of ET can be observed.

Keywords Soil moisture · Evapotranspiration · Solar radiation · Interactions · Central Africa · Reanalysis datasets

1 Introduction

In recent decades, Land–atmosphere interactions have received increasing attention (e.g. Koster et al. 2004; Wei and Dirmeyer 2010; Liu et al. 2014), revealing an impressive range of Land–atmosphere coupling strengths (Lawrence and Slingo 2005). Changes in local physical processes, such as soil moisture-atmosphere interactions, have been identified as driving factors of climate variability and change (Seneviratne et al. 2006; Vidale et al. 2007). Soil moisture (SM) is one of the most important sources of atmospheric predictability (Guo and Dirmeyer 2013), as antecedent SM significantly influences the onset, duration, and intensity of extreme events (e.g., floods, droughts, and heat waves) (Lorenz et al. 2010; Alexander 2010; Seneviratne et al. 2010; Quesada et al., 2012; Ho-Hagemann et al. 2015). SM is also key to the impact of the Land–atmosphere coupling on climate through the limitation of evapotranspiration (ET) (Seneviratne et al. 2010).

A comprehensive evaluation of a region's hydrological and water cycles requires the integration of surface soil moisture (SSM) and root-zone soil moisture (RZSM) data. These two land surface variables are fundamental to

✉ Ellen Dyer
ellen.dyer@ouce.ox.ac.uk

1 Laboratory for Environmental Modelling and Atmospheric Physics (LEMAP), University of Yaounde 1, Yaounde, Cameroon

2 Department of Physics, Higher Teacher Training College, University of Yaounde 1, Yaounde, Cameroon

3 School of Geography and the Environment, University of Oxford, Oxford, UK

4 School of Geographical Sciences, University of Bristol, Bristol, UK

Published online: 20 February 2026

regulating the hydrological cycle (Peng et al., 2021; Srivastava et al., 2013). SSM—which supplies water for direct evaporation (Jaksa and Sridhar, 2015)—plays a pivotal role in enhancing the understanding, modelling and prediction of climate-related processes. In contrast, RZSM—representing the water accessible to vegetation roots—is indispensable for practical applications such as irrigation planning and drought assessment (Jaksa and Sridhar, 2015; Sadri et al., 2020). This consideration is particularly salient in densely forested regions such as Central Africa (CA), where plant transpiration, predominantly sustained by root-zone water uptake, constitutes a significant source of atmospheric moisture. Moreover, within the context of global warming, the projected increase in atmospheric water vapour is generally associated with increased ET over land—despite notable regional disparities—which may subsequently lead to declining SM levels (IPCC AR6 WGI Report, Chapter 8; Douville et al. 2021). ET is also recognised as a crucial process for examining the feedback mechanisms between SM content and precipitation dynamics (e.g. Liu et al. 2014). Notably, regions with high levels of surface and root-zone SM, such as CA, have been identified as falling within an energy-limited ET regime, where radiation and energy availability rather than SM itself primarily constrain ET (Koster et al. 2004; Guo and Dirmeyer 2013).

The understanding of the surface energy balance and the coupling with land surface water involves considering the interaction between SM content (SSM and RZSM) and ET. ET represents the energy transferred from the land to the atmosphere. It is also the main pathway by which water moves from the ground to the atmosphere. According to Dirmeyer et al. (2000) and Entekhabi et al. (1996), SM is the main driver of the land surface water and energy balance coupling. Thus, changes in total evaporation reflect changes in the flux of moisture at the Land–atmosphere interface, which is another important aspect of the Land–atmosphere coupling. Therefore, characterisation of the ET regime is concerned with determining how strongly the SSM and RZSM constrain land ET and the resulting feedback to the atmosphere (Haghighi et al. 2018).

In CA, a region where more than 20% of precipitable water comes from local ET (Pokam et al. 2012; Dyer et al. 2017), extreme and unpredictable rainfall events are becoming increasingly common. The strong flow of moisture from ET highlights the role of Soil moisture-Evapotranspiration Interactions (SEIs) in the occurrence and intensity of extreme events in CA, and may be highly sensitive to local land surface processes. Deng et al. (2020) identified a significant proportion of CA as having experienced a substantial decrease in soil moisture levels between 1979 and 2017. This drying trend intensified between 2001 and 2017 and has been linked to accelerated changes in land use and land cover across CA, particularly between 2010 and 2020 (Nahayo et al. 2023). Together, these observations reflect rapid changes in SEIs, suggesting an acceleration in regional climate change. Furthermore, the projected reduction in total wet-day rainfall in CA (Fotso-Nguemo et al. 2019) strengthens the likelihood of a connection between SEI changes and the supply of atmospheric moisture. Given that soil moisture—especially in the root zone—governs plant water uptake for transpiration, its decline may serve as a precursor to drought, thereby threatening regional water availability (Sridhar et al., 2008).

Despite its ecological importance, CA has received relatively limited attention in efforts to understand SEIs. Most studies that have addressed SEIs have been conducted at global or continental scales (Koster et al. 2004; Mwanthi et al. 2023), but these may not capture the region's unique dynamics. These studies have demonstrated the strong dependence of model results on their initial parameterisation (Mwanthi et al. 2023), highlighting the non-transferability of initial SM conditions across models (Koster et al. 2004). Furthermore, the ability of these models to accurately represent the complex climate of CA remains controversial, as none of these studies have included a regional assessment of the mechanisms likely to influence the ability of SM anomalies to induce changes in ET anomalies. Creese and Washington (2016, 2018) assessed the performance of regional and global models simulating CA climate, emphasising the need for improved representation of physical processes. Consequently, the role of SSM and RZSM in modulating the partitioning of incoming radiation into sensible and latent heat—ultimately shaping temperature and humidity in the lower atmosphere—remains an open question in this region.

This study presents a multi-year evaluation of the strength and nature of SEIs in CA. The primary objective is to examine the role of SM—both SSM and RZSM—in driving the variability of ET. Additionally, we investigate the local drivers of spatio-temporal variability of ET based on an assessment of possible interactions between SSR and SSM/RZSM, which may induce changes in ET rates. Throughout this analysis, particular emphasis is placed on soil moisture types in relation to the amount of water available for ET across the region. With this in mind, our ultimate goal is to identify the underlying mechanisms of SEIs specific to each soil moisture type. Achieving these objectives will allow us to address the following questions: To what extent does SM drive the spatiotemporal variability of ET in CA? What role does SSR play in shaping this variability? The definition of the regional mechanisms of ET, taking into account the influence of these key components of Land–atmosphere feedback, can inform model development and evaluation.

The scarcity of observational data in CA has increased over the past three decades (e.g., Washington et al. 2013; Asefi-Najafabady and Saatchi 2013; Zhou et al. 2014; Nicholson et al. 2018). As a proxy, the global gridded reanalysis products are widely used to understand the regional climate and its response to large-scale disturbances. Two of these reanalysis datasets will be used in this study. We compare the ability of MERRA2 and ERA5 to satisfactorily reproduce energy transfer at the Land–atmosphere interface.

This study is structured as follows: a presentation of the data and methods used in Sect. 2, followed by the presentation and discussion of the results (Sect. 3), and a conclusion summarising the main findings and implications of the study (Sect. 4). Section 3 includes the analysis of the nature and strength of SEIs within each soil moisture type (Sect. 3.1), the investigation of the temporal evolution of land surface and atmospheric parameters involved in SEIs (Sect. 3.2), and the combined influence of evergreen forest and cloud cover on complex SEIs (Sect. 3.3). The study concludes with an assessment of the controls of changes in SM and SSR on wet and dry season ET variability (Sect. 3.4).

2 Data and methods

2.1 Data

This work compares the ability of multiple reanalysis datasets to satisfactorily capture the SEIs using monthly data from two reanalyses from 1980 to 2020. While both datasets use data assimilation techniques to provide improved estimations by optimally integrating land surface models, they have different strengths.

The first reanalysis dataset, ERA5-Land, is provided by the Copernicus Climate Change Service (C3S) of the European Centre for Medium-Range Weather Forecasts (ECMWF). It offers high-resolution land surface data with a spatial resolution of $0.1° \times 0.1°$, enabling detailed analysis of continental water and energy fluxes. ERA5-Land is a refined version of the fifth generation European ReAnalysis (ERA5) global dataset, with an improved resolution of about 9 km that provides finer insights into land surface variability (Muñoz-Sabater et al. 2021).

The second reanalysis dataset used is MERRA-2, produced by the National Aeronautics and Space Administration (NASA) Global Modelling and Assimilation Office (GMAO). It provides monthly mean two-dimensional land surface data, a valuable resource for examining Land–atmosphere interactions (Gelaro et al. 2017).

Along with these two datasets, the 2012–2020 daily high-resolution Level 3 (L3) descending soil moisture data (V001) with 0.25° grid resolution generated by the Advanced Microwave Scanning Radiometer 2 (AMSR2) using the Land Parameter Retrieval Model (LPRM) algorithm (Kachi et al. 2013; Yao et al. 2021; Xing et al. 2021) are also included in this study as a reference. By using microwave radiation, the AMSR2 satellite instruments provide data independent of the visible and infrared observations used by MERRA2 and ERA5. In a cloudy region like CA, this is very valuable for cross-validation and availability of data regardless of cloud cover.

SSM provided by MERRA2 and AMRS2 is the moisture content measured in the 0–5 cm soil layer, while that from ERA5-Land is measured in the 0–7 cm soil layer. The moisture content at the depths of 0–7 (θ_{7cm}), 7–28 (θ_{28cm}), and 28–100 cm (θ_{100cm}) was used to compute the weighted average of the 0–100 cm RZSM from ERA5-Land using the following definition from Xing et al. (2021), which is derived from that of González-Zamora et al. (2016):

$$\theta_{rzsm} = 0.07 * \theta_{7cm} + 0.2 * \theta_{28cm} + 0.72 * \theta_{100cm}. \quad (1)$$

MERRA2 provides RZSM directly at a depth of 0–100 cm.

Table 1 provides a detailed list of all the variables that we used in this study.

2.2 Methods

2.2.1 Clustering methods

Our study focuses on Central Africa: 15° S–15° N and 7° E–35° E. CA has shown spatial heterogeneity in the variability of precipitation (e.g., Dezfuli 2017; Camberlin et al. 2019), and temperature (e.g., Aloysius et al. 2016; Fotso-Nguemo et al. 2017) and evaporation (e.g., Crowhurst et al. 2021; Worden et al. 2021). In this context, climate regionalisation appears to be a valuable tool for partitioning such heterogeneous regions into homogeneous subregions based on single or multiple climatic variables. We perform a clustering of our study area using the K-means method applied to the evaporative fraction (EF), which is calculated using the definition of Santenello et al. (2011). The EF classifies soil conditions from dry to freely evaporating surfaces, with values ranging from 0 to 1 (Santanello et al. 2011). As a key indicator of energy partitioning at the Land–atmosphere interface, the EF is valuable for estimating ET (Liu et al. 2020). Consequently, clustering the study area based on EF prior to assessing SEIs enhances the accuracy of our analysis of the dependence of ET variability to spatio-temporal changes in land surface variables such as SSR, SSM and RZSM.

K-means clustering is a non-hierarchical, unsupervised machine learning algorithm used to partition data points into a pre-defined number (K) of clusters based to their proximity to cluster centroids (Wilks 2011). Its ability to identify patterns

Table 1 Summary of the variables used in this study

Dataset	Variables	Spatial resolution (lon x lat)	Temporal resolution	Period
ERA5-Land	Total evaporation; Soil water content layer 1, 2 and 3; Surface net solar radiation; 2 m temperature; Total precipitation; Total cloud cover; Leaf area index; Surface latent heat flux; Surface sensible heat flux	0.1° × 0.1	Monthly	1980–2020
MERRA2-Land	Total evaporation; Surface soil moisture; Root zone soil moisture; Surface net solar radiation; 2 m temperature; Total precipitation; Total cloud cover; Leaf area index; Surface latent heat flux; Surface sensible heat flux	0.625° × 0.5°	Monthly	1980–2020
†AMSR2	Level 3 (L3) descending soil moisture data (V001)	0.25° × 0.25°	Daily	2012–2020

without prior labeling makes it particularly suitable for regionalization using climate data. By applying K-means to the EF, we identified distinct zones within the study area—hereafter referred to as soil moisture types—based on the availability of soil water to support ET. Each cluster delineates a homogeneous region, which is ideal for examining indirect Land–atmosphere coupling processes through the assessment of SEIs.

To address the seasonal variability of CA's climate, clustering was performed on the seasonal mean EF across the four standard seasons. This enabled the spatial partitioning of EF into clusters representing similar seasonal SM availability for sustaining ET. The optimal number of clusters was determined using both the Silhouette score (Rousseeuw 1987) and the Elbow method (Thorndike 1953).

2.2.2 Statistical tools and significance

Composite methods were employed in this study to examine the variability in ET rates caused by changes in SM. To assess statistical significance, the bootstrap algorithm (Efron 1979; 1982) was applied to composite ET anomalies for years with positive, negative and neutral SM conditions. This algorithm is based on a random sampling method (Varian, 2005). In this study, the resampling procedure was performed with replacement using Monte Carlo simulations. The mean test statistic was calculated for each replicate and the resulting values were used to determine the upper and lower 95% confidence bounds. These bounds were defined by the 2.5th and 97.5th percentiles across all bootstrap replicates. The observed ET anomalies were then filtered using these confidence bounds, representing the expected range of statistical variability due to sampling. Any data points falling outside the confidence interval were considered unreliable and excluded during filtering. Therefore, the filtering criteria were defined to remove all values outside this interval.

In addition to the bootstrap approach, a two-tailed Student's t-test was used to evaluate the statistical significance of the correlation coefficients and both the terrestrial and atmospheric coupling indices. Based on t-statistics, the likelihood that the observed associations occur by chance was determined using *p*-values. A 95% confidence level was used for this analysis. As with the bootstrap method, a filtering criterion was applied to the results. The same t-test procedure was also implemented in the trend analysis.

3 Results and discussion

3.1 Nature and strength of soil moisture-evapotranspiration interactions

3.1.1 Seasonal mean spatial patterns of soil moisture types

The significant seasonal difference in ET rates observed in the Congo Basin (CB) (Crowhurst et al. 2021; Worden et al. 2021, 2024) implies a seasonal consideration in the clustering of our study area. Therefore, in order to best describe and represent the mean seasonal variation in the nature and strength of SEIs, and to further investigate the seasonal effects of SM content on this interaction, k-means clustering is applied to the EF from MERRA2 and ERA5 for each season. Using both the elbow diagram and the silhouette score,

agreement was found on an optimal number of four clusters between the two reanalyses.

Figure 1 shows the spatial distribution of the seasonal mean EF, clustered into four soil moisture types based on the amount of moisture available for ET: very wet, wet, dry, and very dry soils. The four soil moisture types show a zonal distribution that undergoes a meridional migration throughout the four seasons. The two reanalyses agree that of the four soil moisture types, the very wet area is the largest in CA. This soil moisture type, located on average between 3°N and 14°S, migrates northwards from DJF (Fig. 1a and e) to JJA (Fig. 1c and g), followed by a southward shift in SON (Fig. 1d and h). This northward shift is accompanied by a marked reduction in the spatial extent of very wet area, with its northernmost location in JJA corresponding to the maximum spatial extent of dry soils. The observed meridional migration of the very wet soil zone across CA is consistent with the seasonal march of the rain belt over Africa described by Nicholson (2018), and may indicate the positive feedback between SM and precipitation (Sun and Wang 2012).

Considering DJF and MAM seasons, the southern part of CA (15°S-5°N) experiences a wet soil regime (e.g., very wet and wet areas), consistent with the finding of Mwanthi et al. (2023), and the northern part (5°N-15°N) experiences a dry soil regime (e.g., dry and very dry areas). During JJA and SON seasons, dry soil regimes are observed both north and south of the wet soil regime. As a result, the spatial seasonal pattern of wet, dry and very dry soils appears to depend on the seasonal migration of very wet soils across the region. The overall heterogeneity of CA in terms of the spatial seasonal distribution of SM available for ET may lead to different responses of ET to changes in SM in different sub-regions.

3.1.2 Seasonal variation in direction and magnitude of soil moisture-evapotranspiration interactions

To assess the direction and strength of the SEIs, correlation analysis (Lou et al. 2022) is used to examine the relationships between ET, SM and SSR. Seasonal mean correlation coefficients are calculated for each soil moisture type for MERRA2 and ERA5. The cluster spatial means and standard deviations are shown in Fig. 2. While both datasets show positive correlations between ET and SSM/RZSM, ET and SSR exhibit positive and negative correlations (see Fig. 2a–d and m–q). However, the strength of the correlation and the standard deviation vary greatly across soil moisture types.

In the very wet area, ET shows weak positive correlations ($r < 0.5$) with SM and SSR across all seasons (see Fig. 2a and m). Similarly, both datasets also display weak values for the terrestrial and atmospheric coupling indexes (TCI and ACI; Dirmeyer 2011) (see Fig. 2j–k and v–w). The standard deviations are high, with ERA5 displaying more dispersion than MERRA2. Generally, both datasets show stronger correlations between ET and SSM/RZSM than with SSR, except for ERA5 in DJF (see Fig. 2a). This suggests that SSM and RZSM may influence ET more than SSR. However, given comparable coefficient of determination (r^2) values between ET–SSM/RZSM and ET–SSR (Fig. 2e and q), SM and SSR may concurrently influence ET variability. Nevertheless, as all r^2 values are below 50%, less than half of ET variability is explained by any single factor. This indicates that SEIs in this area are likely to be positive but weak according to Zhang et al. (2008). In contrast, in wet area, ET shows strong, positive correlations with SSM and RZSM across all seasons, with low standard deviations (see Fig. 2b and n). Conversely, the correlations between ET and SSR are weaker, negative and exhibit greater dispersion.

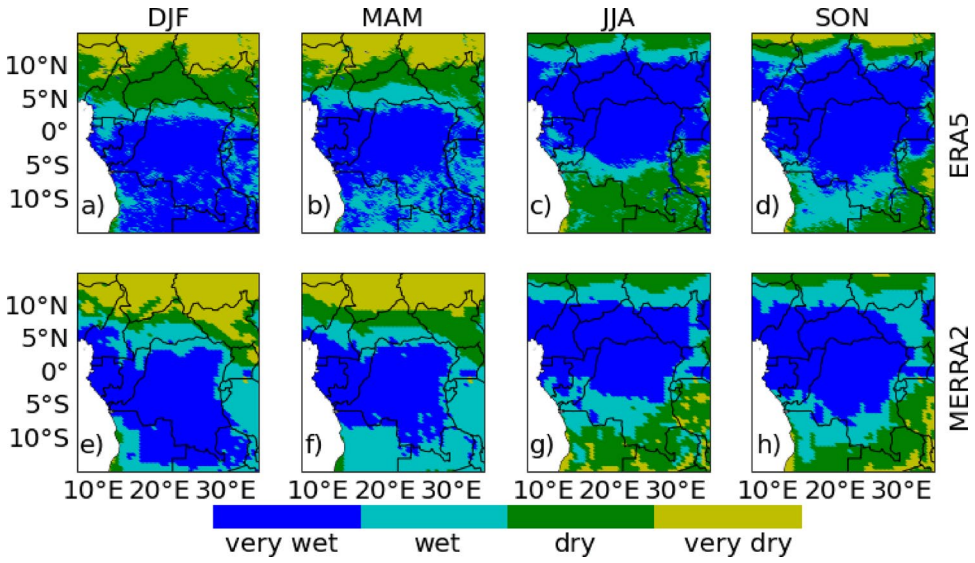

Fig. 1 K-means clustering of the seasonal average spatial distribution of the four soil moisture types (very wet soil, wet soil, dry soil, and very dry soil) using the evaporative fraction from ERA5 (**a**, **b**, **c**, and **d**) and MERRA2 (**e**, **f**, **g**, and **h**) over the period 1980–2020 in CA

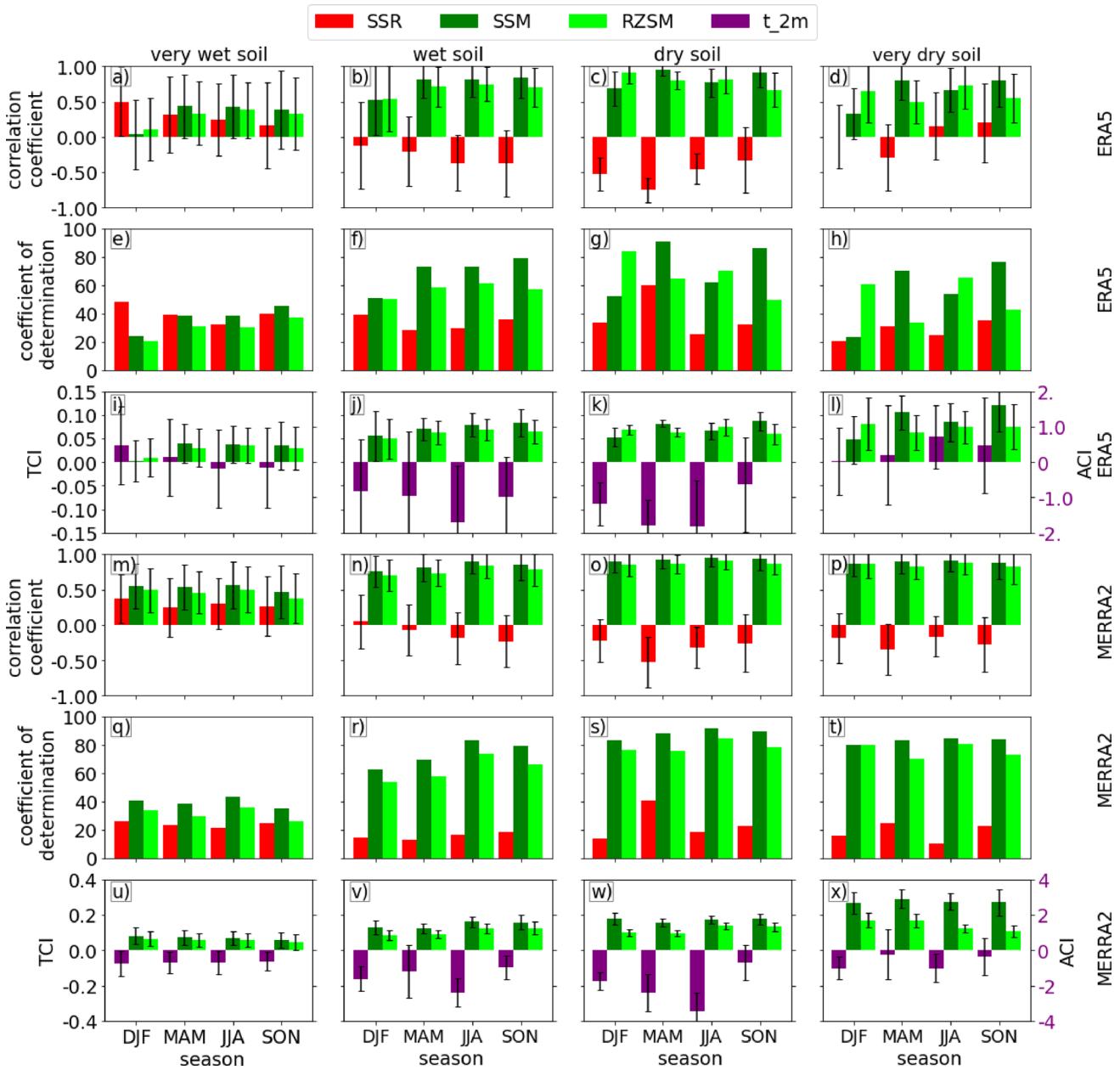

Fig. 2 Seasonal spatial averages of various metrics presented across the four soil moisture types. (a–d and m–p) Correlation coefficients between ET and SSR (red bars), SSM (forest green bars) and RZSM (lime green bars). (e–h and q–t) Corresponding coefficients of determination. (i–l and u–x) Seasonal mean values of the ACI and TCI. The TCI is derived using latent heat flux in combination with either the SSM (forest green bars) or the RZSM (lime green bars), while the ACI is computed using latent heat flux and the 2-metre air temperature (t_2m, purple bars). Data are derived from ERA5 (top three rows) and MERRA2 (bottom three rows). All metrics are computed over the period 1980–2020 and the error bars indicate the standard deviation.

Furthermore, r^2 values for ET–SSM/RZSM consistently exceed 50%, whereas those for ET–SSR remain well below (see Fig. 2f and r). This suggests that SM exerts a stronger influence on ET variability than SSR.

In dry soil regimes (i.e. dry and very dry areas), both datasets exhibit strong positive correlations between ET and SSM/RZSM, with minimal standard deviation (see Fig. 2c–d and o–p). ERA5 exhibits greater sensitivity of ET to SSM during wet seasons (MAM and SON) and to RZSM during dry seasons (DJF and JJA). This suggests a shift in ET control from surface to root zone SM during dry periods (see Fig. 2c–d). The groundwater-supported ET is consistent with the findings of Condon et al. (2020) and is not captured by MERRA2 (see Fig. 2o–p). Instead, MERRA2 shows SSM and RZSM as the dominant ET modulators across all soil regimes. SSM generally drives more ET variability than

RZSM, which aligns with the findings of Kim et al. (2023). Overall, MERRA2 reflects a stronger SM-driven ET regime than ERA5. While SM has a strong influence on ET variability, both MERRA2 and ERA5 also show a moderate impact from SSR. In dry area, ET and SSR exhibit a moderate negative correlation across seasons, whereas in very dry area, the correlations are weaker and more mixed. Compared to SSM and RZSM, the lower r^2 values for SSR suggest a weaker influence on ET (see Fig. 2g–h and s–t). This is likely because, although net solar radiation can control ET through its influence on temperature variation (Zhang et al. 2015), this control appears to be stronger in humid forests (Kim et al. 2023).

The stronger correlations between SM and ET revealed by both datasets in the transitional areas compared to the very wet area align with the TCI patterns. However, the TCI appears to be highest in very dry area, consistent with increased SM control over ET as SM content decreases, according to Kim et al. (2023). This apparent SM-driven ET regime in some clusters—which contrasts with the conclusions of Mwanthi et al. (2023) on CA's hydrometeorological—may partly explain the significant discrepancies observed in atmospheric general circulation models (AGCMs) employed in previous Land–atmosphere coupling studies (e.g. Koster et al. 2004, 2006; Lorenz et al. 2015). For example, half of the 12 AGCMs in the Global Land–Atmosphere Coupling Experiment (GLACE) project identified CA as a hotspot for Land–atmosphere coupling (Koster et al. 2004). Nevertheless, Dirmeyer et al. (2006) observed that AGCMs tend to underperform in modelling land–atmosphere interactions at local to regional scales.

The lower dispersion of correlation scores and the stronger SM-driven ET regime displayed by MERRA2 compared to ERA5 is consistent with the discrepancy observed in the seasonal spatial distribution of correlation scores, ACI and TCI, between the two datasets (see Fig. S1). However, both datasets show agreement regarding lower standard deviation in transitional areas than in areas of extreme soil moisture (very wet and very dry areas), as well as lower TCI and ET-SM correlation dispersions than ACI and ET-SSR correlation dispersions. The two datasets also agree on the coincidence of regions of strong positive influence of SM on ET with regions of strong negative influence of SSR on ET (Fig. S1). This feature is associated with two strong opposite patterns of relative sensitivity of ET for all metrics in ERA5 and is consistent with the findings of Abdolghafoorian and Dirmeyer (2021). They observed that regions with a strong influence of SM variations on latent heat flux also have strong negative correlations between SM and sensible heat flux. Furthermore, the low dispersion of values and the greater sensitivity of ET variability to SM in MERRA2 compared to ERA5 appear to be associated with a dominant spatial pattern of ET sensitivity to SM variability rather than to SSR variability in all seasons and for all metrics in MERRA2. The greater dispersion of values in extreme soil moisture areas compared to transitional areas (Fig. 2) is associated with the combined positive or negative influence of SM and SSR on ET, particularly in very wet area (Fig. S1).

3.1.3 Impact of soil moisture-solar radiation interaction on the direction and magnitude of soil moisture-evapotranspiration interactions

The previous section showed the potential for a combined SSR and SM to influence ET in some areas. Here, we use the partial correlation coefficient to isolate the true relationship between SM and ET, as well as between SSR and ET. This enables us to analyse the effect of SM (or SSR) on ET while controlling for the effect of SSR (or SM) (Anderson 1984). The results are shown in Fig. 3.

Both datasets show substantial improvements in correlation scores and r^2, as well as a significant reduction in dispersion of values in the very wet area (Fig. 3.a-b and 3.c-d). The improvement of the correlations between ET and SSR when the effect of SM is excluded indicates that SSR's influence on ET depends heavily on SM content. The same is true for the influence of SM on ET. This suggests that there may be some feedback between SSR, SM and RZSM, consistent with previous studies establishing a link between SSR and variation in SM content (e.g. Zhang et al. 2001, 2018; Atchley & Maxwell 2011; Song et al. 2012). Atchley and Maxwell (2011) and Zhang et al. (2001) found that ET was the bridge of this interaction. However, the influence of SSR on ET appears to be more sensitive to SM content in the surface layer than in the root zone layer. Zhang et al. (2017) found that radiative energy affects soil evaporation and tree transpiration differently; this helps to explain why SSR has a contrasting impact on SEIs in the surface and root zone layers. The strength and direction of the influence of SM on ET seem to depend on SSR, and vice versa.

In other areas, the interaction between SSR and SM mainly affects the direction of SSR's influence on ET. The two datasets show an inversion of the correlation between ET and SSR in wet, dry and very dry soil (see Fig. 3, first and second columns). This is evident in the change from a negative to a positive correlation when the influence of SSM and RZSM are excluded. However, this inversion is accompanied by a slight change in the magnitude of the correlation. Consequently, SM exerts a dual influence on the nature and strength of the effect of SSR on ET in these regions. This suggests that the negative correlation between SSR and ET observed in Fig. 2 may be the result of a negative feedback loop between SM and SSR. Consistent with

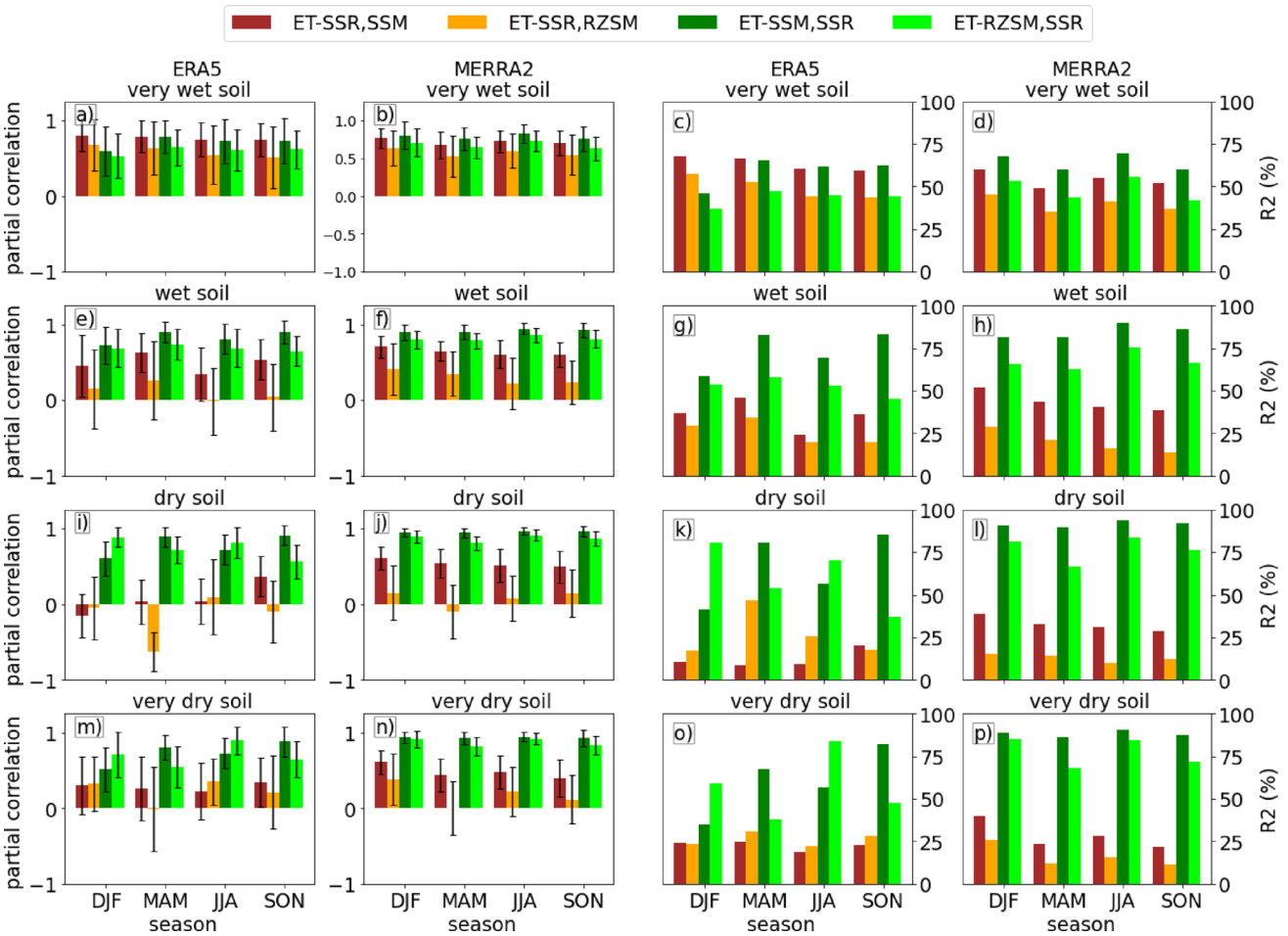

Fig. 3 Seasonal spatial averages of partial correlation coefficients shown across four soil moisture regimes. Brown bars represent the partial correlation between ET and SSR while controlling for SSM. Orange bars show the partial correlation between ET and SSR while controlling for RZSM. Forest green and lime green bars show the partial correlations between ET and SSM and ET and RZSM respectively, while controlling for SSR. The first and second columns display these partial correlation values from ERA5 (a, e, i, m) and MERRA2 (b,f, j, n), respectively. The third and fourth columns show the corresponding coefficients of determination respectively for ERA5 (c, g, k, o) and MERRA2 (d, h, l, p). All metrics are calculated for the period 1980–2020, with error bars showing the standard deviation

observations in very wet area, this feedback appears to be relatively weaker in the root zone than in the surface layer (particularly evident in MAM).

Nevertheless, MERRA2 still shows a greater influence of SSM on ET than RZSM. Without the effect of SSR, it also fails to capture the competitive control between SSM and RZSM on ET during wet and dry seasons (see Fig. 3l and p). Overall, the influence of SSM and RZSM on the magnitude of the influence of SSR on ET is less uniform outside the very wet area. Overall, across soil moisture types, it can be seen that SM and SSR can inhibit or enhance their respective influences on ET, which may result in complex SEIs, particularly in very wet area.

3.2 Temporal evolution of land surface and atmospheric parameters involved in the soil moisture-evapotranspiration interactions

3.2.1 Trends analysis and relation with the soil moisture-evapotranspiration interactions

To investigate how differences in the nature and strength of the SEIs can affect the average variation in ET induced by SSM, RZSM and SSR, Fig. 4 shows the spatially averaged trends in ET, SSM, RZSM and SSR from MERRA2 and ERA5. MERRA2 and ERA5 are in agreement only in the very wet area, with decreasing (increasing) trends in ET, SSM and RZSM (SSR) in all seasons (Fig. 4a, b). DJF is an exception to the discrepancy in the trend of SSR between the two datasets in wet (Fig. 4c, d), dry (Fig. 4e–f), and very dry (Fig. 4g, h) areas.

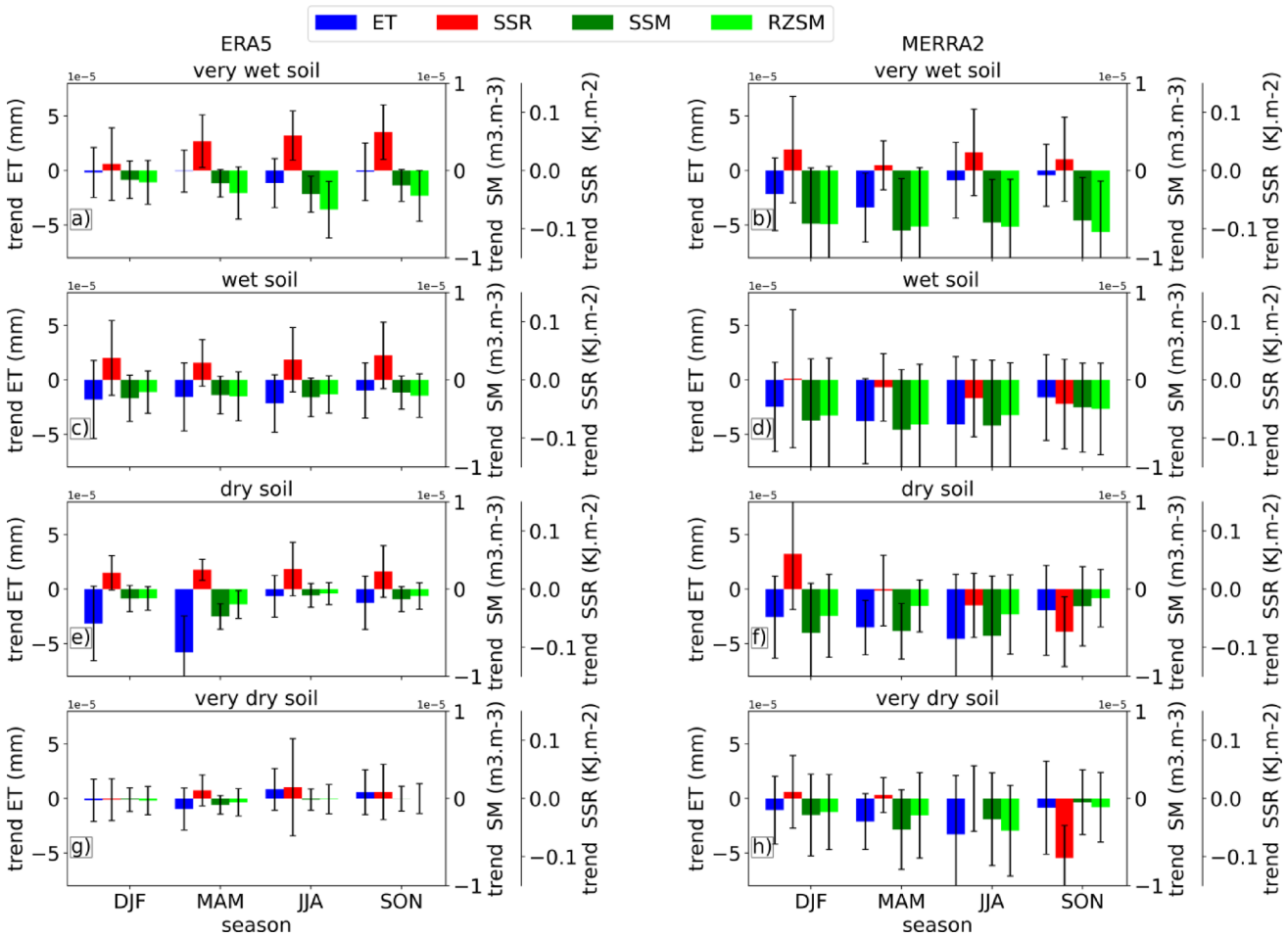

Fig. 4 Seasonal spatial averages in the four soil moisture types of the trend in ET (blue bars), SSR(red bars), SSM (forest green bars) and RZSM (lime bars) from ERA5 (a, c, e, g) and MERRA2 (b, d, f, h) for the period 1980–2020 in CA. Standard deviationsare represented by error bars

However, the trends of ET in all seasons and clusters differ markedly—in both direction and magnitude—from the significantly increasing global trend of 0.88 mm yr-2 reported by Zhang et al. (2015) for the period 1982–2013. In contrast, the decreasing trend of SM across CA, as shown in both reanalysis datasets, aligns with the global soil drying documented in earlier studies (Albergel et al. 2013; Deng et al. 2020). Deng et al. (2020) identified this region as a hotspot of long-term SM drying (1979–2017), and observed that the strong persistence of SM drying indicates that CA soils will continue to be dominated by a drying trend in the future. Given that increases in SM typically boost latent heat flux and thus ET (Jaksa and Sridhar, 2015), a decline in SM is also likely to suppress ET. Therefore, The consistently decreasing ET trend observed across all clusters in both ERA5 and MERRA-2 supports the hypothesis that SM exerts a stronger influence on ET than SSR in this region.

Figure 4 also shows that the changes in ET could be induced by both changes in SM and SSR. The influence of the modulator is the largest, so the ET trend will follow that of the modulator. However, if two modulators can exert the same influence on ET and have opposite trends, then the ET trend will be the smallest and will follow that of the modulator with the greatest variation. The smallest ET trends from ERA5 and MERRA2 provide two examples of this (Fig. 4a and b). Since SM and SSR exert contrasting influence on ET in the very wet area, the smallest trend in ET from ERA5 and MERRA2 is recorded in this area. The weakest decreasing trend of ET in MAM is consistent with the combined increasing and decreasing trends of SSR and SSM and RZSM (Fig. 2a).

The strongest decrease in ET in the same season in dry area is also consistent with this explanation (Fig. 4e). The strong influence of SM on ET in the dry area is associated with a moderate but significant influence of SSR (Figs. 2; S1). Therefore, the moderate negative and positive trends in SM and SSR, respectively, result in a strong negative trend in ET, as indicated by ERA5. This implies that if two modulators driving opposite changes with the same strength in ET have opposite trends, the trend in ET is assumed to be the

strongest. Conversely, if they have opposite trends and can influence ET in the same way, the ET trend is assumed to be the weakest. However, if a variable is not a modulator of ET, the ET trend may not be related to that of the variable. For example, ET shows a moderate decreasing trend in the very wet area, despite a strong increasing trend in SSR (see Fig. 4a). These findings align with the hypothesis proposed by Teuling et al. (2009) that regional trends in land evaporation are responsive to trends in the limiting drivers. Furthermore, the extent to which a specific driver exerts control over the evaporation process enables the prediction of long-term changes in evaporation, given changes in the controlling factor (Miralles et al. 2011; Jaksa and Sridhar, 2015).

Although ERA5 accurately represents this pattern, the trends shown by MERRA2 may appear somewhat confusing. However, MERRA2 also show a strong correlation between the trends in SM and ET, indicating a significant influence of SM on ET (Fig. 4, right panel). Furthermore, the spatial pattern of the ET trend appears to be more consistent to that of SSM and RZSM (not shown), as observed in the spatial seasonal mean.

Overall, the transitional areas, which can be classified in a moisture-limited ET regime, show a pronounced sensitivity of ET trends to trends in SM compared to trends in SSR (Fig. 4c–f). In the very wet area, which was assumed by Mwanthi et al. (2023) to have an energy-limited ET regime due to the weak influence of the surface soil water content on ET variability, the trend of ET is sensitive to that of both SM and SSR. On a seasonal average, spatially statistically significant ($p<0.01$), decreasing (increasing) trend patterns of ET well match decreasing (increasing) trend patterns of SM (SSR) in both datasets (not shown). This suggests the potential for a moisture-limited ET regime, rather than an energy-limited ET regime, in this area, as the dependence of ET on SSR is observed to be relatively limited when compared to the dependence of ET on SM, and also when considering the feedback between SSR and SM revealed in Sect. 3.1.3. This is consistent with the reservations expressed by Koster et al. (2004) regarding the intuitive energy-limited hydro-meteorological regime of the CA. Consequently, further analysis is required to elucidate the hydrometeorological regime of the CA, particularly in the context of climate change, where there is a strong likelihood of prolonged and continuous soil drying in this region (Deng et al. 2020).

3.2.2 Study domain average annual and interannual variability of land–atmosphere parameters.

Figure 5 shows the annual cycle and interannual variability of land surface atmospheric variables as derived from ERA5 and MERRA2, in addition to data on SM from both reanalyses and an observational dataset, namely AMSR2. Bimodal patterns are observed for ET, SSR and RZSM from ERA5 and MERRA2 (Fig. 5a). Furthermore, both ERA5

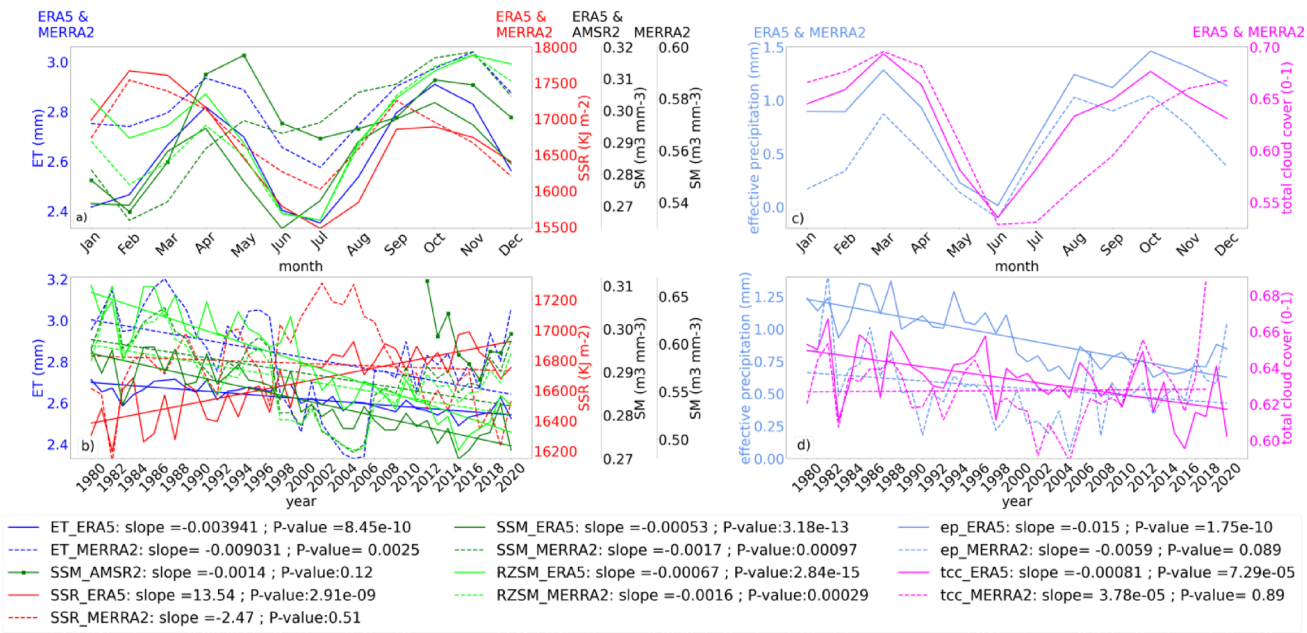

Fig. 5 Spatially averaged annual (**a** and **c**) and interannual (**b** and **d**) variability of land surface parameters from ERA5 (solid line) and MERRA2 (dashed line) over CA for the period 1980–2020. The AMSR2 soil moisture level 3 dataset (SSM_AMSR2) for the period 2012–2020 is used as the reference for the soil moisture products from MERRA2 and ERA5 comparisons. The second Y-axis (on the right side of plots **a** and **b**) shows both SSM and RZSM values from ERA5 and the soil moisture values from AMSR2. The third Y-axis shows only the SSM and RZSM values from MERRA2. The effective precipitation presented in this study is the difference between rainfall and evapotranspiration

and AMSR2 show a bimodal pattern of SSM, in contrast to MERRA2. The difficulty in representing the two annual peaks in SSM may be related to the overestimation of both SSM and RZSM by MERRA2 compared to AMSR2 and ERA5 (Fig. 5a, b). The systematic overestimation of SM by MERRA2 is consistent with its underestimation of effective precipitation compared to ERA5 (Fig. 5c). This characteristic of MERRA2 has also been observed in previous studies (Igbawua et al. 2019; Kenfack et al. 2023). As reported by Igbawua et al. (2019), this discrepancy may be due to imbalances resulting from adjustments in data assimilation methods, satellite calibration and observational databases.

The extreme wetness of MERRA2, is related to the influence of SM on effective precipitation. In fact, higher SM leads to more water available for direct evaporation from the soil surface, as well as for plants to take up and return to the atmosphere through transpiration (Jaksa and Sridhar, 2015). Excessive transpiration and evaporation increases the rate of ET, which ultimately reduces the amount of water remaining as effective precipitation. In addition, the already elevated SM content of MERRA2 may be associated with a higher total ET rate compared to ERA5, resulting in delayed drying cycles. The prolonged drying period due to the high estimated SM content extends the period of enhanced ET and its impact on the atmosphere, explaining the inability of MERRA2 to capture the June/July minimum in SM (Fig. 5a).

A direct consequence of the dependence of SM memory on soil depth is the competitive control of ET variability by surface and root zone SM during wet and dry seasons observed in dry and very dry areas in the ERA5(Figs. 2, S1). The ET water supply in the ERA5 is comparable to the findings of Lion et al. (2017), who observed a difference in ET water supply between surface and deeper soil layers during wet and dry seasons, respectively. The failure of MERRA2 to capture this phenomenon may be due to the characteristics of this dataset, which tends to overestimate SM content. This in turn has the direct consequence that SM from MERRA2 induces more changes in ET than SSR compared to ERA5.

A negative trend is observed for ET, SSM and RZSM from ERA5 and MERRA2 over the period 1980–2020 (Fig. 5b). All trends are statistically significant ($p<0.01$). This significant decreasing trend of ET, SSM and RZSM is consistent with the decreasing trends observed in each soil moisture type (Fig. 4). The regional agreement of a dominant soil drying in CA is consistent with the findings of previous studies (e.g. Jung et al. 2010; Deng et al. 2020) and the regional significant decreasing trend of ET is also consistent with the average strong influence of SM on ET variability. Conversely, this agreement serves to accentuate the contrast with the global significant increasing trend observed by Jung et al. (2010) and Zhang et al. (2015), but strongly agrees with the regional exceptions of ET increase in arid areas reported in the IPCC AR6 report (Douville et al. 2021).

Meanwhile, as observed on an annual cycle (Fig. 5a), MERRA2 shows an excess of up to 0.19 $m^3.m^{-3}$ of soil water content compared to ERA5. This is consistent with the deficit of effective precipitation in MERRA2 compared to ERA5 (Fig. 5d). The two reanalyses show a negative trend over the study period with a significant difference in values (MERRA2: -0.0059 mm/year, $p=0.089$; ERA5: -0.015 mm/year, $p<0.01$). This deficit is also observed in the ET trends between the two datasets over the study period (MERRA2: -0.009 mm/year, $p<0.01$; ERA5: -0.0039 mm/year, $p<0.01$). However, there is a large discrepancy between the datasets during the period 1998–2008. MERRA2 shows a strong decrease in ET rates, consistent with the trends in SSM and RZSM, and a strong increase in SSR compared to ERA5. These patterns have been observed in previous studies and may be associated with the transition to El Niño conditions, according to the results of previous studies (e.g. Jung et al. 2010; Miralles et al. 2014; Zhang et al. 2015), but are not captured byERA5. After this strongly decreasing period, the ET rate from MERRA2 shows a slightly increasing trend during the period 2008–2020 where the ET rate from ERA5 shows a continuously decreasing trend.

Figure 5 also shows a discrepancy in the SSR trends of ERA5 and MERRA2 over the study period, with an increasing trend for the former and a decreasing trend for the latter (MERRA2: -2.47 $kJ.m^{-2}$/yr, $p=0.51$; ERA5: 13.54 $kJ.m^{-2}$/yr, $p<0.01$). This discrepancy is consistent with the opposite trend in total cloudiness (Fig. 5d), which is decreasing and increasing for ERA5 and MERRA2, respectively (MERRA2: $3.78\times10–5$/year, $p=0.89$; ERA5: -0.0081/year, $p<0.01$). These divergent trends, and the MERRA2 increasing trend in total cloud cover (TCC) also observed by Wu et al. (2022), may be due to the period of strong increasing trend that occurred in the period 1998–2008 in response to the decrease in SM and ET. In fact, this period is followed by a strong decrease in the trend of SSR, and this may explain the weak decreasing trend in SSR averaged over the study period (-2.47 $kJ.m^{-2}$/year) from MERRA2 compared to the strong positive trends from ERA5 (13.54 $kJ.m^{-2}$/year). Furthermore, the two datasets agree well on increasing trends in SSR until 2005, which is consistent with the global increase in radiative energy found by Wild et al. (2008) over the period 1986–2000.

Overall, on a spatial average over the study area, the trend of ET over the study period, as in each soil moisture type, appears to follow the decrease in SM. This result is consistent with the drying observed by Zhang et al. (2015), but also indicates that the CA ET interannual variability may be

strongly modulated by ENSO, according to Miralles et al. (2014). Assuming the intensification of the El Niño-driven drying observed by Power et al. (2013), CA is expected to experience continuous drying conditions in the future. Therefore, the resulting SM limitations on ET, as depicted by Jung et al. (2010), could sustain the decreasing trend of ET, indicating a potential moisture-limited hydrometeorological regime.

The seasonal spatially averaged interannual variability shows decreasing trends in ET, SSM and RZSM from ERA5 and MERRA2 that persist in all four seasons over the study period (Fig. S2). In addition, the discrepancy between MERRA2 and ERA5 in the trends in SM and ET shown on the annual average over the period 1998–2008 is also visible at the seasonal scale. This suggests that these decreases in MERRA2 SM and ET rates occurred throughout the year over the period 1998–2008. However, as with the annual mean, the seasonal means of the spatially averaged interannual variability of SSR show a significant discrepancy between MERRA2 and ERA5. In contrast to the trend in ET and SM, there is an opposite trend in SSR in almost all seasons (except the DJF) between MERRA2 and ERA5. Both ERA5 and MERRA2 exhibit increasing SSR trends in DJF that align with corresponding decreases in TCC, echoing findings by Jaksa and Sridhar (2015). However, during the rainy seasons, MERRA2 reveals an apparent inconsistency: while SSR decrease, TCC does not show the expected increase.

Nevertheless, this seasonal analysis further strengthens the consistency of a regional decrease in ET in CA, resulting from an SM limitation, with the persistent regional drying observed by Deng et al. (2020).

3.3 Very wet area cloud cover and evergreen forest combined impact on complex soil moisture-evapotranspiration interactions

3.3.1 Soil moisture-evapotranspiration interactions and composite anomaly of evapotranspiration in CA.

To further investigate the variability in ET rate induced by changes in SM, the effects of SSM and RZSM anomalies on the ET anomaly are assessed using the composite anomaly of ET for years of positive, negative, and neutral SM anomalies. Positive (negative) SM anomalies are defined for domain-averaged values of standardised anomalies ≥ 1 (≤ -1) and values between -1 and 1 are considered neutral anomalies.

Figure 6 shows a spatially heterogeneous response of ET to changes in SM content across the seasons in the study area. ET is more sensitive to changes in SM content in some areas, with two contrasting patterns of both positive and negative anomalies. A zone of strong positive sensitivity of ET variability to changes in SM content is located in the northern part of the CB for years of positive (negative) SM anomaly. However, in addition to the primary zone of pronounced positive sensitivity of ET to SM, there is also a distinct pattern in the coastal region, particularly evident in DJF for the year of the positive (negative) anomaly of SM (Figs. 6a-d).

The southern region exhibits a relatively weak and negative response of ET to changes in SM. These two contrasting patterns in the spatial distribution of the composite ET anomalies are evident throughout the year, with a meridional migration of the zonal band of highest positive sensitivity of ET to changes in SM. As a consequence of this migration, the band of highest anomaly is at its most northerly position in JJA (Fig. 6m–p). A second band of strongly positive SEIs is observed in the southwest of the Democratic Republic of Congo (DRC). The two bands show a southward shift in SON. The appearance of this second band in the south is consistent with the northerly location of the very wet area (Fig. 1). Consequently, the transition zones show the strongest positive sensitivity of ET variability to SM content, a finding consistent with the highest correlation values observed (Fig. 2). Similarly, the weak negative sensitivity of ET to SM variability is also consistent with the lowest correlation scores.

The spatial heterogeneity of the ET response to changes in SM associated with the seasonal migration of the zonal band of very wet area, along with the seasonal shift of the belt of the strong positive response of ET to SM changes, suggests the existence of a seasonal hydrometeorological regime transition across the study area. Moreover, using the feedback efficiency (Zhang et al. 2008), the soil moisture anomalies leading evapotranspiration anomalies by one month is assessed. All the patterns shown by the composite anomaly of ET are also visible in the spatial distribution of the seasonal and annual mean of the feedback efficiency of SM on ET in both the surface and root zone layers (Fig. S4; S5). Thus, some areas could transition from an energy-limited to a moisture-limited state, while others transition from a moisture-limited to an energy-limited state throughout the year. Furthermore, Denissen et al. (2022) have shown that the most pronounced shift from energy to water limitation occurs in regions exhibiting both increasing and decreasing trends in net radiation and SM, respectively. This pattern, which is clearly visible in CA (see Figs. 4 and 5), combined with the significant soil drying trend, could lead to a more permanent transition in the hydrometeorological regime in this region.

The seasonal spatial average of the composite anomaly of ET for years with positive, negative and neutral anomalies of SM shows a considerable dispersion of values in

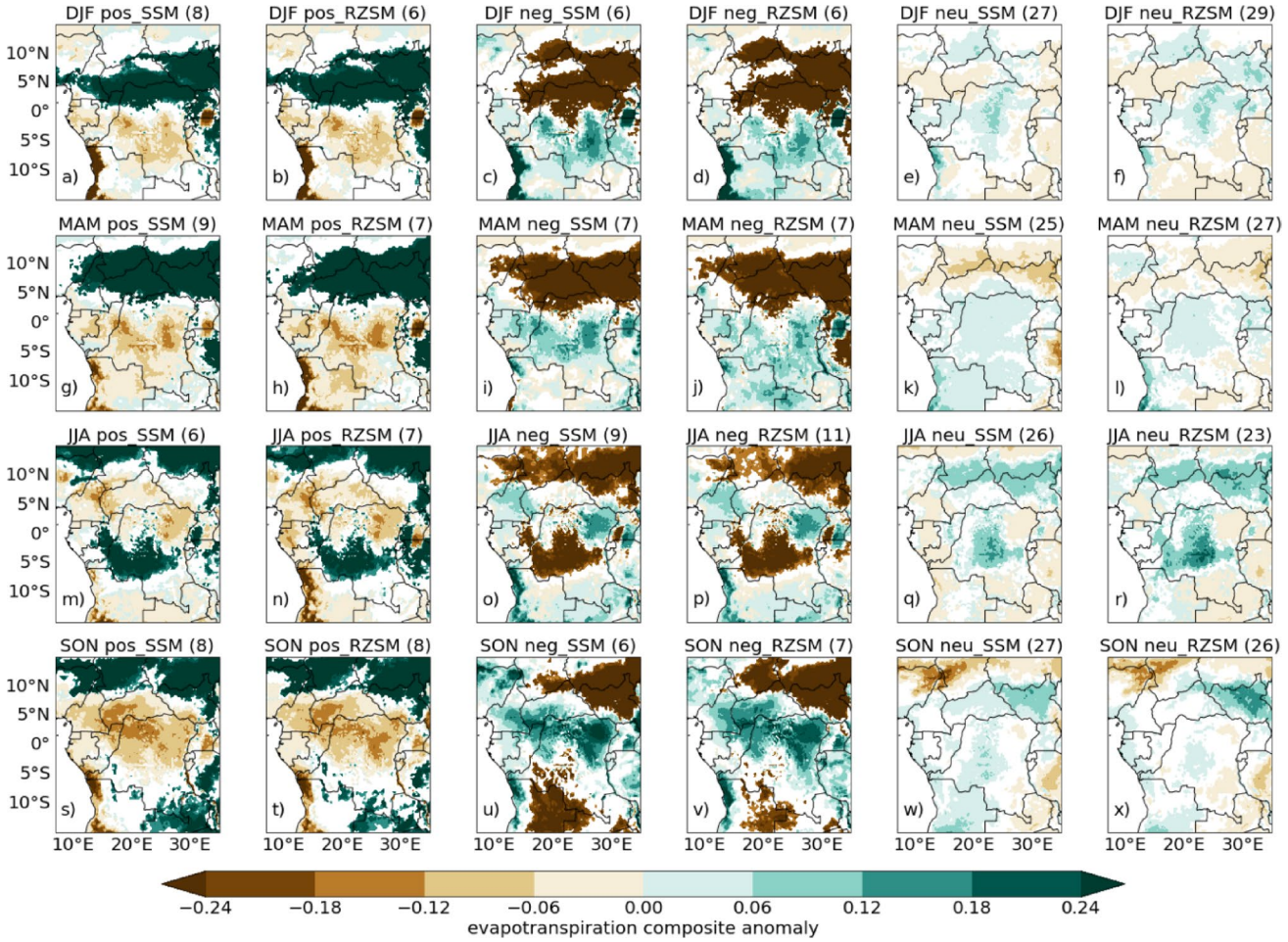

Fig. 6 Seasonal spatial distribution in the composite anomaly of total evaporation for years of positive (a, g, m, s) first column and (b, h, n, t) second column), negative (c, i, o, u) third column and (d, j, p, v) fourth column) and neutral (e, k, q, w) fifth column and (f, l, r, x) sixth column) anomaly of SSM and RZSM for the period 1980–2020 in CA. Years of positive (respectively negative) anomalies are considered as those with standard anomaly values > 1 (respectively < − 1) and neutral years for values in [− 1,1]. A statistical significance test at the 95% confidence level is applied to the total evaporation composite anomaly using bootstrapping. The present plot is based exclusively on data from ERA5 reanalysis

very wet area (Fig. 7). This is probably due to the significant heterogeneity in the spatial distribution of the ET anomaly in this area, which is indicative of a complex SEI. The spatial distribution of years with a neutral SM anomaly is more homogeneous. Furthermore, there is a lack of consensus regarding the magnitude of the change in ET induced by changes in SM across seasons. This discrepancy extends to the direction of change induced when extreme positive anomaly values are considered. Indeed, in MAM an average negative anomaly in ET is observed for years with strong positive SM anomaly. The ET anomaly for years with a neutral SM anomaly is low and positive for each season, and as for years with extreme anomaly values, the highest anomaly values are recorded in JJA. These observations, coupled with the apparent stronger response of ET anomalies to negative than positive SM anomalies, align with the predominant soil drying. Additionally, the spatial distribution of SM anomalies in years with strong positive (negative) mean SM anomalies is more homogeneous than that of ET (see Fig. S3). This suggests a possible impact of biophysical factors on SEIs, and plant transpiration, which depends on environmental conditions and is driven by RZSM (Anderson et al. 2012), may be a key channel of SEIs in very wet area.

3.3.2 The role of leaf area index and cloud cover on SEIs.

To assess the combined effect of evergreen forest and permanent cloud cover on SEIs, Fig. 8 shows the spatial distribution of the seasonal mean of the leaf area index and total cloud cover in CA. The leaf area index shows a quasi-permanent distribution across seasons. The highest values are observed in the northern region of the DRC. This pattern observed in the two datasets is associated with a slight reduction in the area of the highest values during the dry

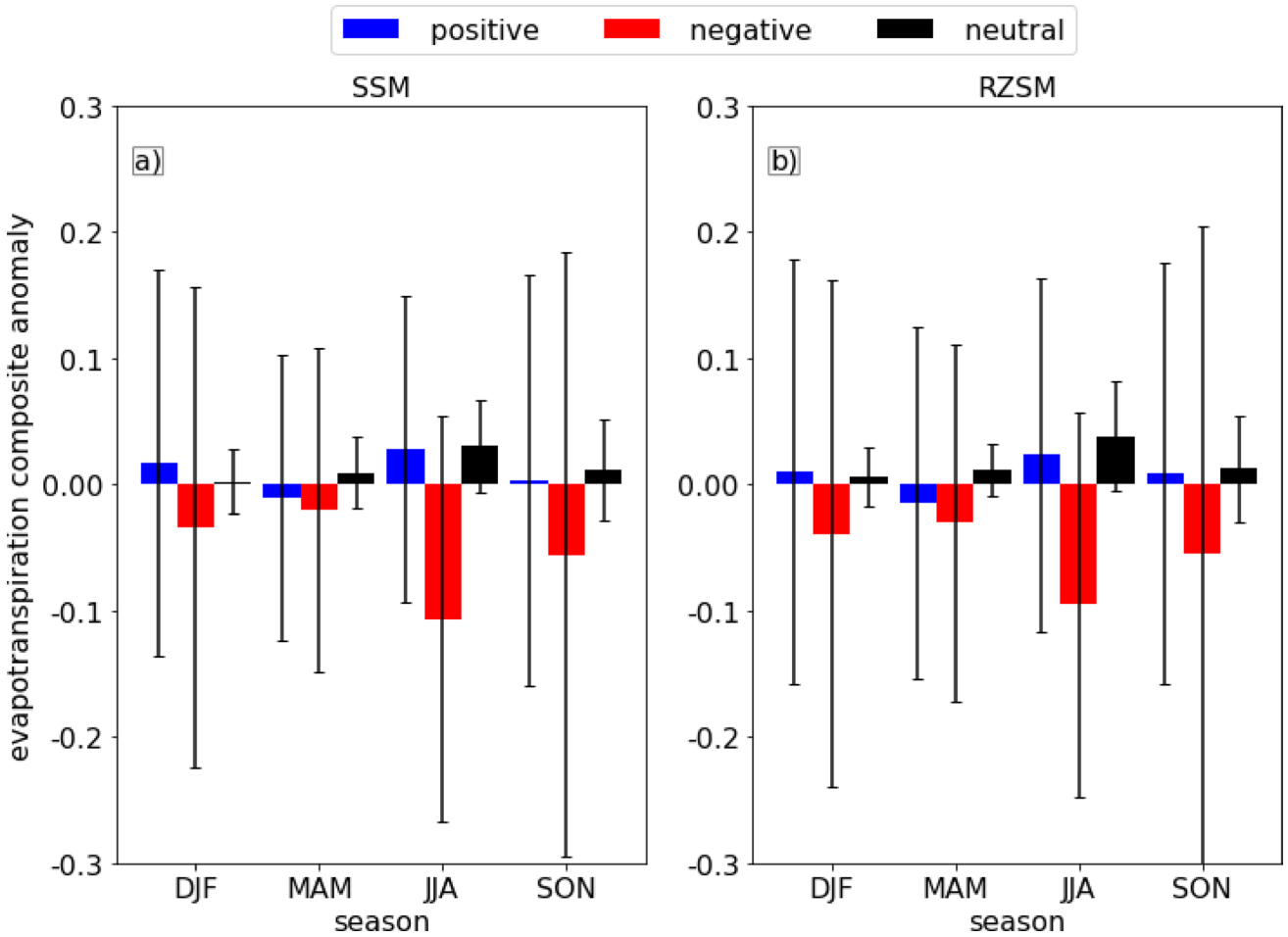

Fig. 7 Seasonal spatial average in very wet area of the composite anomaly of evapotranspiration for years of positive, negative and neutral anomaly of SSM (**a**) and RZSM (**b**) over the period 1980–2020. Positive (or negative) anomaly years are those with standard anomaly values > 1 (or < −1) and neutral years are those with values in [−1,1]. Standard deviations are represented by error bars

season (JJA). Consequently, these values are almost exclusively located in very wet area (Fig. 8a–h). Furthermore, it appears that the area with the highest cloud cover over the study area is also located in the area of high leaf area index in each season of the year (Fig. 8i–p). Consequently, very wet area shows a robust association between evergreen forests and high cloudiness, which is consistent with the findings of Cerasoli et al. (2021) that forested areas globally tend to occupy regions with higher cloud fractions.

Thus, the very wet area is the location of both permanent clouds and evergreen forests, and these two factors together may have a complex and interesting effect on the SEIs. Transpiration from evergreen forests is a major contributor to the total amount of ET in CA according to Crowhurst et al. (2020). The location of high leaf area index in very wet area suggests that SM could have a significant effect on ET variability, assuming that SM in the root zone is the main driver of plant transpiration (Anderson et al. 2012; Song et al. 2017). On the other hand, SSR has been found to be a driver of ET in evergreen forests (Song et al. 2017), and tree transpiration appears to be an important pathway through which SSR drives ET (Song et al. 2017; Lion et al. 2017). For example, Lion et al. (2017) observed that plant roots are the primary cause of soil drying below field capacity, as soil evaporation decreases rapidly with depth. Similarly, Brooks et al. (2010) found that water with the longest residence time in the soil is more likely to be removed by plants and not discharged to streams during dry periods.

Furthermore, forests absorb more SSR than savannahs due to lower reflectivity, resulting in more transpiration than soil evaporation (e.g. Zhang et al. 2017; Cerasoli et al. 2021). In addition, the greater cloud cover in forest areas than in savannahs (Cerasoli et al. 2021), which are almost in transitional areas, suggests a greater cloud feedback on SEIs in forest areas (very wet area). Consequently, the contribution of SSR to ET depends on tree transpiration in very wet forest areas, which is consistent with the strong correlation between transpiration and ET found in the humid tropics (Zhang et al. 2017). Thus, both SSR and RZSM influence changes in total evaporation from plant transpiration in very

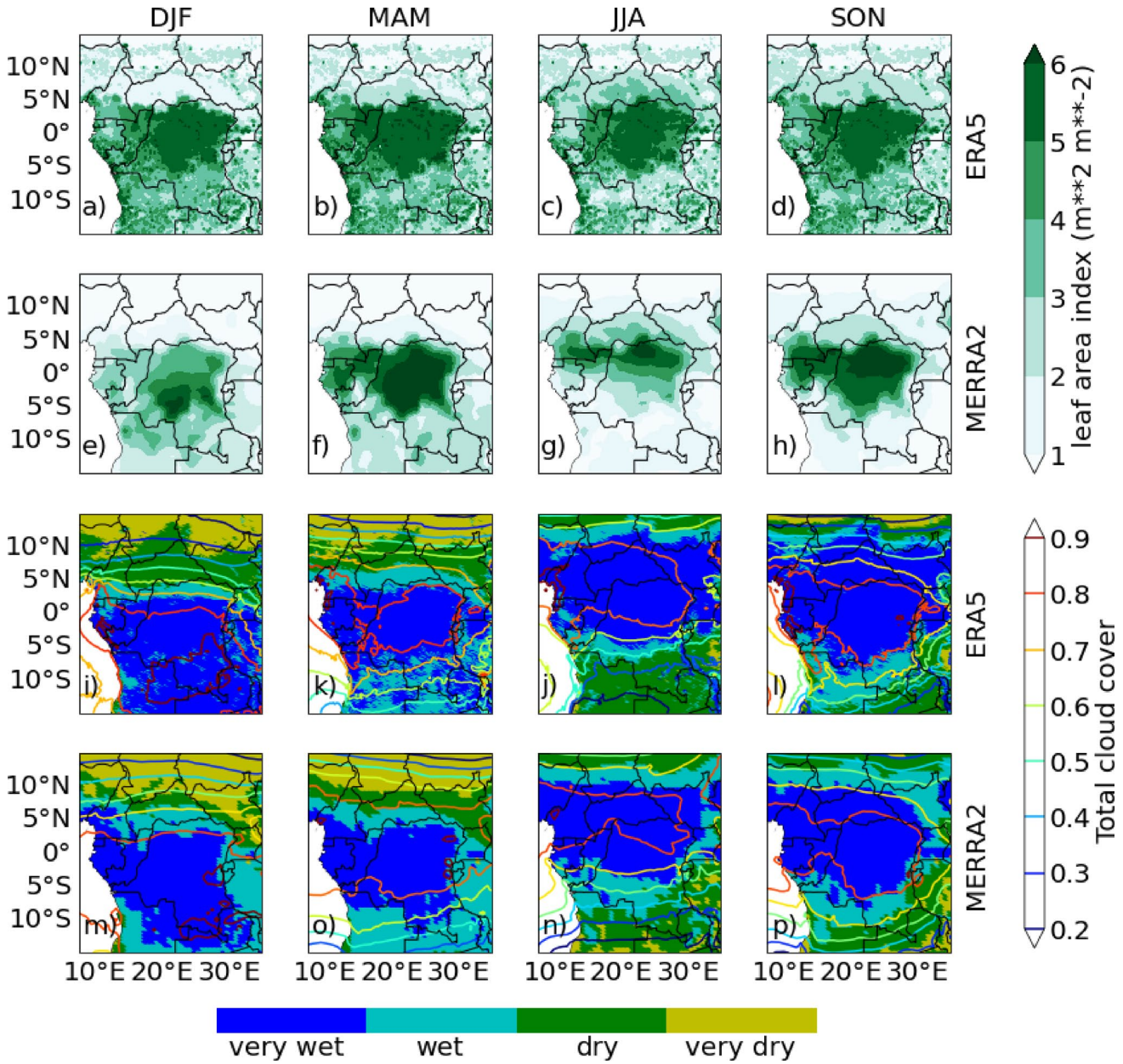

Fig. 8 Seasonal spatial distribution of: (a–h) leaf area index, (i–p) K-means clustering of the four soil moisture types (very wet soil, wet soil, dry soil and very dry soil) using evaporative fraction (in shade) and total cloud cover (in contour) from ERA5 (a–d and i–l) and MERRA2 (e–h and m–p) over the period 1980–2020 in CA

wet area with evergreen forests. In Amazonia, for example, radiative energy has been found to be an important contributor to interannual variability in transpiration and consequently ET (Zhang et al. 2017). However, high cloud cover combined with forest is also expected to create a cooler and wetter environment (Cerasoli et al. 2021). Indeed, through the process of tree transpiration, energy is expensive to cool surface air, limiting surface heating (Denissen et al. 2021). This may have led to a reduction in ET according to (Kanniah et al. 2013). However, the large amount of moisture from ET observed in previous studies (Crowhurst et al. 2020) may have mitigated the reduction in SSR, resulting in a high ET rate. This explains the slightly higher value of the correlation between ET and SM compared to SSR in each soil moisture type (Fig. 2).

Overall, very wet area appear to be under both moisture-limited and energy-limited ET regimes. As an indicator, the variability of ET is driven by changes in SM and radiative energy through the strong dependence of transpiration on both. Zhang et al. (2017) used the definition of McVicar et al. (2012) to classify Equatorial Central Africa into an equitant climate regime. Thus, this region lies between the

two boundaries of moisture-limited and energy-limited ET regimes. However, the discrepancy observed between the two reanalysis datasets with regard to the contribution of SM to ET variability, as well as the magnitude of changes in land surface variables over the study period, is fairly consistent with the variation across datasets reported by Hirschi et al. (2025) and Nogueira (2020) in their analysis of soil-drying and rainfall trends. While these previous studies revealed fairly good agreement between ERA5/ERA5-Land and ground measurement datasets (e.g. the European Space Agency Climate Change Initiative (ESA CCI) product and the Global Precipitation Climatology Project (GPCP)), significant differences were observed between the outputs of MERRA2 and those of both ERA5 and observational datasets. This highlights the need for an observation-based investigation into the interaction between SM and ET to validate this hypothesis. Meanwhile, the spatiotemporal gaps in measurement data, which are exacerbated in CA by biophysical factors such as high cloudiness and dense vegetation, highlight the need to consider the choice of observational data when investigating soil moisture–atmosphere feedback.

Moreover, local moisture recycling plays a critical role in Central Africa's hydrological cycle (as highlighted by Pokam et al. 2012; Dyer et al. 2017). The important changes in land use and land cover that have occurred in CA between 1990 and 2020 (Nahayo et al. 2023), may have played a critical role in this process. For example, they may have accelerated soil drying and decreased evapotranspiration rates. Consequently, the wettest CA region is expected to transition to a moisture-limited climatic regime in the future. The ecosystem limitation index (ELI; Denissen et al. 2022), based on the difference between ET-SM and ET-SSR correlations, shows a stronger upward trend in this region. This indicates that the most significant transition is occurring in the very wet area (Fig. S6). In the context of a changing climate—associated with a decrease in ET and SM, and an increase in SSR in CA (see Figs. 4 and 5)—it is crucial to identify the mechanisms controlling ET under varying SM conditions.

3.4 Controls of soil moisture and surface solar radiation changes on evapotranspiration variability during wet and dry seasons

As shown in previous sections, ET variability is primarily influenced by changes in soil water content, as well as by the interaction between SM and SSR. This highlights the importance of taking a holistic approach that considers the combined effect of SM and SSR when analysing the drivers of ET in CA. Figure 9 focuses on evaluating the sensitivity of ET anomalies to concurrent SM and SSR anomalies at the surface and in the root zone. The analysis is conducted across three distinct regions, highlighted in Fig. 9 0.25–28: ever-wet (persistently saturated, red box); transitional wet (moderate to extreme wetness, purple box); and transitional dry (extreme dryness to moderate wetness, black box).

In the ever-wet area, at the surface layer (see Fig. 9 0.1–4), changes in SSR appear to be the primary contributor to ET variability. This pattern—particularly evident in JJA (see Fig 9 0.3)—is, however, characterised by relatively weak ET changes (anomalies ranging from -0.8 to 0.8), compared to SSR changes. By contrast, at the root zone layer (Fig. 9 0.5–8), ET variability strongly responds to changes in both SM and SSR, consistent with their combined influence on tree transpiration. Meanwhile, in the transitional wet area, the surface and root zone layers exhibit close patterns (see Fig. 9 0.9–16). In JJA and SON, when the purple box covers very wet soil, changes in both SSR and SM significantly contribute to ET variability at the surface and root zone layers. Similarly, in DJF and MAM, when the purple box covers the transitional areas (wet and dry soils), ET variability becomes highly sensitive to SM across both layers, with the role of SSR being less significant. However, in the transitional dry area, changes in SM appear to be the primary contributor to ET variability, regardless of soil depth (see Fig. 9 0.17–24). Nevertheless, under very dry conditions (in DJF and MAM) and in the root zone layer, the ET response to SM weakens compared to in the wetter seasons and in the surface layer, possibly due to water limitations.

These observations emphasise the significant impact of soil water content, which is shaped by the seasonal migration of very wet soil, on the seasonal sensitivity of ET variability to changes in SM and SSR. However, the weak changes in ET in response to SSR anomalies at the surface layer, compared to the root zone layer, observed in ever-wet area, could be linked to interception by plant leaves (Madhumali et al. 2024), reflecting a combined radiative and moisture-driven regime rather than radiative control of ET. This aligns with the combined effects of radiation and SM on transpiration in evergreen rainforests (Costa et al. 2010) and highlights plant transpiration as the primary contributor to total ET in ever-wet regions (Costa et al. 2010; Miralles et al. 2011; Peters 2016). The lower surface albedo resulting from dense vegetation in this area (see Fig. 8) likely reduces ET variability at the surface, whereas greater variability in the root zone layer could indicate an equitant climate regime, as suggested by Zhang et al. (2017). Nevertheless, this assumption of an equitant climate regime revealed by ERA5 could be more a result of the data used than the real climatic characteristics of CA. A reconsideration of this hypothesis using MERRA2, which indicates a consistent tendency for SSM to control ET variability, would likely support a water-driven climate regime. This overestimation of the sensitivity of ET variability to changes in SM by MERRA2,

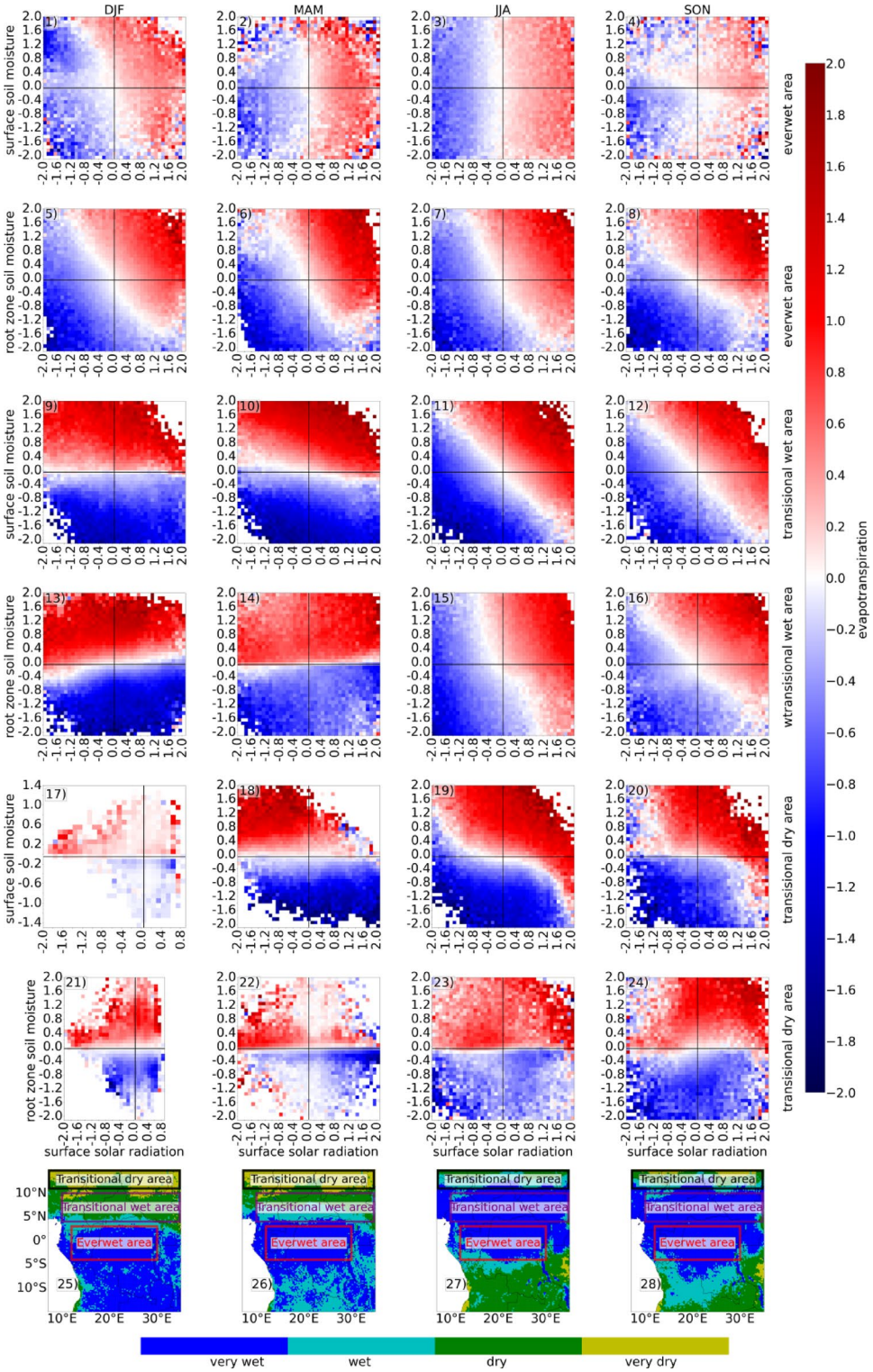

Fig. 9 Water versus energy control of evapotranspiration variability in Central Africa over the study period (1980–2020). Seasonal mean variation of evapotranspiration anomalies as a function of soil moisture and solar radiation anomalies evolution is presented for region experiencing extreme wet soil condition throughout the year (ever-wet area, red box, Figs. 9. 25–28); the region experiencing a transition from a moderately dry condition to an extremely wet condition (transitional-wet area, purple box, Fig. 9. 25–28) and the region experiencing a transition from an extremely dry soil condition to a wet condition (transitional-dry area, black box, Fig. 9. 25–28). The analysis is conducted for both surface and root zone soil moisture in each of the three selected areas. The present plot is based exclusively on data from ERA5 reanalysis

compared to ERA5, is consistent with its underestimation of soil-drying trends compared to ERA5 and ERA5-Land, as reported by Hirschi et al. (2025). Such examples demonstrate the limitations of using certain reanalysis datasets for the efficient assessment of hydrometeorological regimes and the trends of the variables involved. This is partly due to their difficulty in capturing changes and the various interactions between these land surface variables. Consequently, an observation-based analysis would help improve the accuracy and validity of the hypothesis of an equitant climate regime in CA by strengthening the reliability of the findings

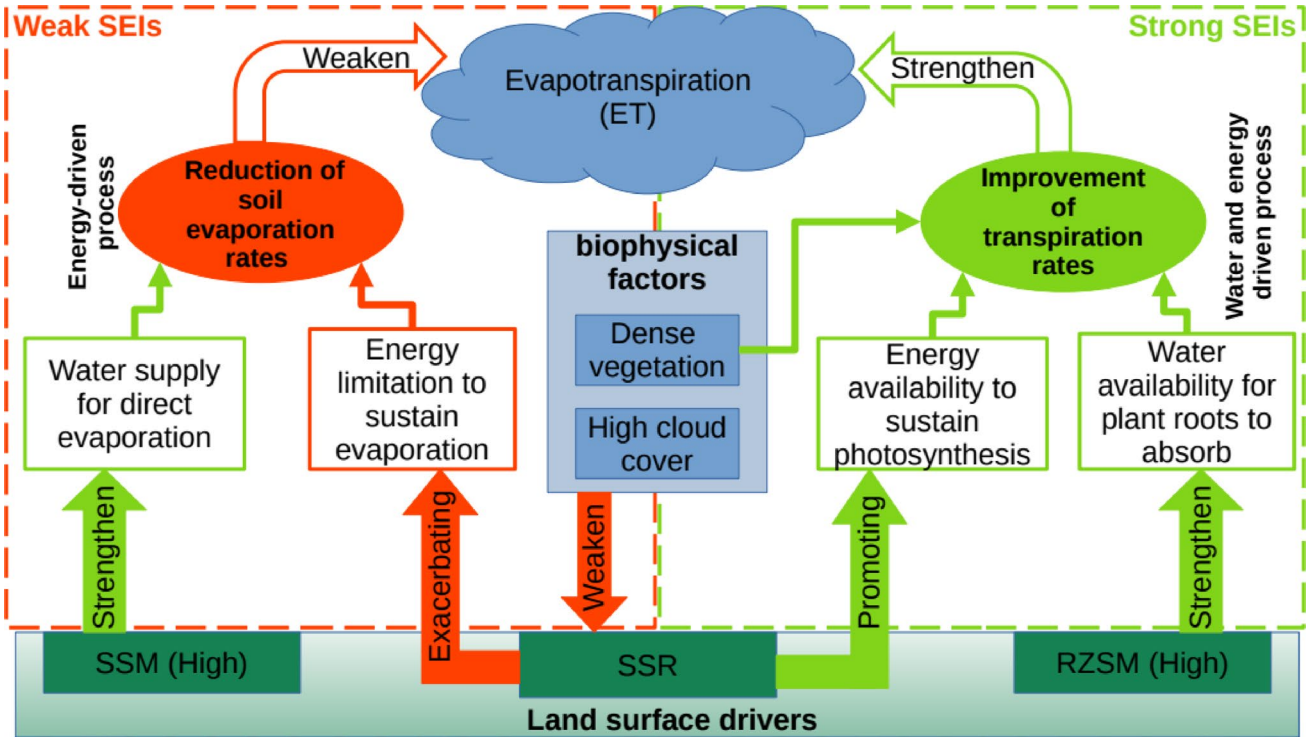

Fig. 10 Schematic diagram of soil moisture-evapotranspiration interactions (SEIs) in very wet soils area. Red arrows indicate a negative contribution of the drivers to the ET process, while lime arrows display a positive contribution. Weak and strong interactions are likely to occur between soil moisture and ET. These interactions involve different levels of soil depth. Despite the strong water supply from the SSM at the surface layer, the limitation of radiative energy induced by high cloudiness and dense vegetation restrains the soil evaporation rate and thus its contribution to ET(weak SEIs). Conversely, the strong water supply from the RZSM combined with dense vegetation, despite the low radiative energy, improves plant transpiration and thus increases its contribution to ET (strong SEIs)

and uncovering nuanced climate patterns that models alone may overlook.

The strong response of ET to changes in SM compared to SSR in transitional dry and wet areas is consistent with the correlation scores (see Fig. 2). This aligns with their location in a hotspot of land–atmosphere coupling (e.g. Koster et al. 2004), and indicates strong positive SEIs, as reflected by the consistently positive ELI observed in these areas, particularly at the root zone layer (Fig. S6). However, according to Jaksa and Sridhar (2015), soil water uptake is faster at the surface than in the root zone due to direct evaporation when vegetation is sparse. This explains why ET variability responds more strongly to SSM than to RZSM in transitional dry area, where limited land and cloud cover, as well as the slower recharge of deep groundwater, enhances ET's sensitivity to available surface soil water.

Three key factors shape the balance between water and energy controls over ET variability: SM content, land cover and cloud cover. High soil water content and land cover induce a contrasting water and radiative control on ET variability between the surface and root zone layers. Cloud cover, meanwhile, directly constrains both radiative and water contributions to ET. High cloud cover reduces evaporative demand, which leads to reduced ET variability. However, water vapour resulting from transpiration, supplied by water and energy, sustains cloudiness in tropical rainforests. In fact, plants produce transpiration via photosynthesis driven by SSR. This plays a critical role in maintaining a high evaporation rate due to the supply of water from the root system. Despite the fact that evaporative cooling would otherwise limit ET.

Overall, the intricate interplay of these factors, particularly in very wet area, creates a complex picture. Figure 10 therefore provides a conceptual framework that synthesises this complex mechanism.

4 Conclusion

This study compared the performance of ERA5 and MERRA2 in capturing and reproducing the SEIs, as well as the contribution of SSR to ET variability in CA. First, we clustered our study area using the K-means method applied to the EF. Then, we assessed the nature and strength of the SEIs by investigating the magnitude and direction of changes in ET induced by changes in SSM, RZSM and SSR. We also assessed the seasonal and SM content dependence of the SEIs.

The main findings of this study are as follows:

1) Based on soil water availability for ET, CA can be categorised into four soil moisture types: very wet, wet, dry and very dry. The very wet area is the largest, and its seasonal migration drives the spatial distribution of the others.
2) SM is the primary driver of ET variability in the transitional areas (wet and dry areas) in both ERA5 and MERRA2, suggesting a water-controlled ET regime. There is a competitive control exerted by SSM and RZSM on ET in the dry soil regimes (dry and very dry areas). SSM dominates ET variability during the wet seasons, while RZSM dominates during the dry seasons. This pattern is captured by ERA5 but not by MERRA2, likely due to MERRA2's tendency to overestimate SM.
3) In the very wet area, ERA5 and MERRA2 show weak correlations between SSR and ET, as well as between SM and ET, which implies complex SEIs. However, analysing the partial correlation score and the impact of biophysical factors reveals a possible interaction between SSR and SM through their contribution to plant transpiration. This interaction influences their relative contribution to ET variability, leading to contrasting radiative and water controls on ET between the surface and root zone layers. Consequently, a complex ET process involving both strong and weak SEIs can be observed (see Fig. 10). This could explain the uncertainty surrounding the hydrometeorological regime of CA, as reported by Koster et al. (2004). While this is consistent with the possibility of an equitant climatic regime, as previously suggested by Zhang et al. (2017), the reanalysis products' difference in ET sensitivity to changes in SSM/RZSM and SSR, alongside reported variations in SM and rainfall trends across datasets (Hirschi et al. 2025; Nogueira et al. 2020), point to regional biases in land surface variables inputs in reanalysis datasets. This demonstrates the need for further observation-based analysis for full validation. However, the difference in results from ground observational products, driven by differences in measurement methods, revealed by Hirschi et al. (2025) in soil drying trend analysis, as well as the spatiotemporal gaps in measurement data in CA, call for caution in choosing the observational dataset for such an assessment.
4) CA is experiencing soil drying, associated with a decrease in ET and an increase in SSR, even in very wet area. Given the weak relative contribution of SSR compared to SM on changes in ET, the intuitive energy-limited hydrometeorological regime of CA is seriously questioned. Moreover, the significant increasing trend in ELI, particularly in very wet area, suggests a possible ongoing transition in the hydrometeorological regime. However, given the discrepancy observed between the two reanalysis datasets used in this study, further investigation using observational data is needed to validate this hypothesis.

The rapid changes in land use and land cover, as reported by Nahayo et al. (2023), combined with the critical role of ET in the region's hydrological cycle, suggest that CA could become more vulnerable to water security risks in the future. As SM influences land-surface energy transfer and is a key driver of ET variability, future research will explore the impact of this meteorological parameter on convective processes. Specifically, the role of SM in shaping the occurrence, intensity, duration and frequency of convection-dependent extreme events such as droughts and extreme rainfall in CA.

Supplementary Information The online version contains supplementary material available at https://doi.org/10.1007/s00382-026-08061-y.

Acknowledgements This work was funded by UK aid from the UK government and by the International Development Research Centre, Ottawa, Canada as part of the PALM-TREEs project (grant no. 110002-002) through the Climate Adaptation and Resilience (CLARE) research programme. The views expressed herein do not necessarily represent those of the UK government, IDRC or its Board of Governors. The authors would like to acknowledge the Copernicus Climate Change Service (C3S) of the ECMWF and the Goddard Earth Sciences Data and Information Services Center (GES DISC) of NASA for providing the reanalysis data used in this study. R. James was funded by a UKRI Future Leaders Fellowship, grant reference MR/W013223/1. The authors would also like to thank the editor and the two anonymous reviewers for their insightful comments, which have greatly helped to improve the manuscript.

Data availability The single-level monthly aggregated land surface data from ERA5-Land, provided by the European Centre for Medium-Range Weather Forecasts (ECMWF), can be downloaded through the Copernicus Climate Change Service (C3S) (https://cds.climate.copernicus.eu/); data from MERRA2 can be accessed through the National Aeronautics and Space Administration (NASA) Goddard Earth Sciences Data and Information Services Center (GES DISC) (https://disc.gsfc.nasa.gov/). Soil moisture data from AMSR2 can also be accessed through the same link.

Declarations

Conflict of interest The authors have no relevant financial or non-financial interests to disclose.

References

Abdolghafoorian A, Dirmeyer PA (2021) Validating the land-atmosphere coupling behavior in weather and climate models using observationally based global products. J Hydrometeorol 22:1507–1523. https://doi.org/10.1175/JHM-D-20-0183.1

Albergel C, Dorigo W, Reichle RH, Balsamo G, de Rosnay P, Munoz-Sabater J, Isaksen L, de Jeu R, Wagner W (2013) Skill and global trend analysis of soil moisture from reanalyses and microwave remote sensing. J Hydrometeorol 14:1259–1277. https://doi.org/10.1175/JHM-D-12-0161.1

Alexander L (2010) Extreme heat rooted in dry soils. Nat Geosci 4(1):12–13. https://doi.org/10.1038/ngeo1045

Aloysius NR, Sheffield J, Saiers JE, Li H, Wood EF (2016) Evaluation of historical and future simulations of precipitation and temperature in central Africa from CMIP5 climate models. J Geophys Res Atmos 121(1):130–152. https://doi.org/10.1002/2015JD023656

Anderson TW (1984) An introduction to multivariate statistical analysis. John Wiley & Sons, United States of America, Canada

Anderson WB, Zaitchik BF, Hain CR, Anderson MC, Yilmaz MT, Mecikalski J, Schultz L (2012) Towards an integrated soil moisture drought monitor for East Africa. Hydrol Earth Syst Sci 16:2893–2913. https://doi.org/10.5194/hess-16-2893-2012

Asefi-Najafabady S, Saatchi S (2013) Response of African humid tropical forests to recent rainfall anomalies. Philos Trans R Soc Lond B Biol Sci 368(1625):20120306. https://doi.org/10.1098/rstb.2012.0306

Atchley AL, Maxwell RM (2011) Influences of subsurface heterogeneity and vegetation cover on soil moisture, surface temperature and evapotranspiration at hillslope scales. Hydrogeol J 19:289–305. https://doi.org/10.1007/s10040-010-0690-1

Camberlin P, Barraud G, Bigot S, Dewitte O, Imwangana FM, Mateso CM, Martiny N, Monsieurs E, Moron V, Pellarin T, Philippon N, Sahani M, Samba G (2019) Evaluation of remotely sensed rainfall products over Central Africa. Q J R Meteorol Soc 145(722):2115–2138. https://doi.org/10.1002/qj.3547

Cerasoli S, Yin J, Porporato A (2021) Cloud cooling effects of afforestation and reforestation at midlatitudes. Proc Natl Acad Sci U S A. https://doi.org/10.1073/pnas.2026241118

Condon LE, Atchley AL, Maxwell RM (2020) Evapotranspiration depletes groundwater under warming over the contiguous United States. Nat Commun 11:873. https://doi.org/10.1038/s41467-020-14688-0

Costa M, Biajoli M, Sanches L, Malhado A, Hutyra L, Rocha H, Aguiar R, de Araújo A (2010) Atmospheric versus vegetation controls of Amazonian tropical rain forest evapotranspiration: are the wet and seasonally dry rain forests any different? J Geophys Res Biogeosci 115(G4):9. https://doi.org/10.1029/2009JG001179

Creese A, Washington R (2016) Using qflux to constrain modeled Congo Basin rainfall in the CMIP5 ensemble. J Geophys Res Atmos 121(22):13415–13442. https://doi.org/10.1002/2016JD025596

Creese A, Washington R (2018) A process-based assessment of CMIP5 rainfall in the Congo Basin: the September–November rainy season. J Climate 31(18):7417–7439. https://doi.org/10.1175/JCLI-D-17-0818.1

Crowhurst DM, Dadson SJ, Washington R (2020) Evaluation of evaporation climatology for the Congo Basin wet seasons in 11 global climate models. J Geophys Res Atmos 125(6):e2019JD030619. https://doi.org/10.1029/2019JD030619

Crowhurst D, Dadson S, Peng J et al (2021) Contrasting controls on Congo Basin evaporation at the two rainfall peaks. Clim Dyn 56:1609–1624. https://doi.org/10.1007/s00382-020-05547-1

Deng Y, Wang S, Bai X, Luo G, Wu L, Cao Y, Li H, Li C, Yang Y, Hu Z, Tian S (2020) Variation trend of global soil moisture and its cause analysis. Ecol Indic 110:105939. https://doi.org/10.1016/j.ecolind.2019.105939

Denissen JM, Orth R, Wouters H, Miralles DG, van Heerwaarden CC, de Arellano JVG, Teuling AJ (2021) Soil moisture signature in global weather balloon soundings. Npj Clim Atmos Sci 4(1):13. https://doi.org/10.1038/s41612-021-00167-w

Denissen JM, Teuling AJ, Pitman AJ, Koirala S, Migliavacca M, Li W, Reichstein M, Winkler AJ, Zhan C, Orth R (2022) Widespread shift from ecosystem energy to water limitation with climate change. Nat Clim Chang 12(7):677–684. https://doi.org/10.1038/s41558-022-01403-8

Dezfuli A (2017) Climate of western and central equatorial Africa. In: Oxford research encyclopedia of climate science. https://doi.org/10.1093/acrefore/9780190228620.013.511

Dirmeyer PA (2011) The terrestrial segment of soil moisture–climate coupling. Geophys Res Lett. https://doi.org/10.1029/2011GL048268

Dirmeyer PA, Zeng FJ, Ducharne A, Morrill JC, Koster RD (2000) The sensitivity of surface fluxes to soil water content in three land surface schemes. J Hydrometeorol 1:121–134.

Dirmeyer PA, Gao X, Zhao M, Guo Z, Oki T, Hanasaki N (2006) GSWP-2: multimodel analysis and implications for our perception of the land surface. Bull Amer Meteorol Soc 87:1381–1397

Douville H, Raghavan K, Renwick J, Allan RP, Arias PA, Barlow M, Cerezo-Mota R, Cherchi A, Gan TY, Gergis J, Jiang D, Khan A, Pokam Mba W, Rosenfeld D, Tierney J, and Zolina O (2021) Water cycle changes. In: Climate change 2021: the physical science basis. Contribution of Working Group I to the sixth assessment report of the intergovernmental panel on climate change [Masson-Delmotte V, Zhai P, Pirani A, Connors SL, Péan C, Berger S, Caud N, Chen Y, Goldfarb L, Gomis MI, Huang M, Leitzell K, Lonnoy E, Matthews JBR, Maycock TK, Waterfield T, Yelekçi O, Yu R, and Zhou B (eds.)]. Cambridge University Press, Cambridge, United Kingdom and New York, NY, USA, pp. 1055–1210, https://doi.org/10.1017/9781009157896.010

Dyer ELE, Jones A, B. D, Nusbaumer J, Li H, Collins O, Vettoretti G, Noone D (2017) Congo Basin precipitation: assessing seasonality, regional interactions, and sources of moisture. J Geophys Res Atmos 122(13):6882–6898. https://doi.org/10.1002/2016JD026240

Efron B (1979) Computers and the theory of statistics: thinking the unthinkable. SIAM Rev 21(4):460–480. https://doi.org/10.1137/1021092

Efron B (1982) The jackknife, the bootstrap and other resampling plans. Society for industrial and applied mathematics

Entekhabi D, Rodriguez-Iturbe I, Castelli F (1996) Mutual interaction of soil moisture state and atmospheric processes. J Hydrol 184(1–2):3–17. https://doi.org/10.1016/0022-1694(95)02965-6

Fotso-Nguemo TC, Vondou DA, Pokam WM et al (2017) On the added value of the regional climate model REMO in the assessment of climate change signal over Central Africa. Clim Dyn 49:3813–3838. https://doi.org/10.1007/s00382-017-3547-7

Fotso-Nguemo TC, Diallo I, Diakhaté M, Vondou DA, Mbaye ML, Haensler A, Tchawoua C (2019) Projected changes in the seasonal cycle of extreme rainfall events from CORDEX simulations over Central Africa. Clim Change 155(3):339–357. https://doi.org/10.1007/s10584-019-02492-9

Gelaro R, McCarty W, Suarez MJ, Todling R, Molod A, Takacs L, Randles CA, Darmenov A, Bosilovich MG, Reichle R, Wargan

K, Coy L, Cullather R, Draper C, Akella S, Buchard V, Conaty A, da Silva AM, Gu W, Kim GK, Koster R, Lucchesi R, Merkova D, Nielsen JE, Partyka G, Pawson S, Putman W, Rienecker M, Schubert SD, Sienkiewicz M, Zhao B (2017) The modern-era retrospective analysis for research and applications, version 2 (MERRA-2). J Clim 30:5419–5454. https://doi.org/10.1175/jcli-d-16-0758.1

González-Zamora Á, Sánchez N, Martínez-Fernández J, Wagner W (2016) Root-zone plant available water estimation using the SMOS-derived soil water index. Adv Water Resour 96:339–353. https://doi.org/10.1016/j.advwatres.2016.08.001

Guo Z, Dirmeyer PA (2013) Interannual variability of land-atmosphere coupling strength. J Hydrometeorol 14:1636–1646. https://doi.org/10.1175/JHM-D-12-0171.1

Haghighi E, Short Gianotti DJ, Akbar R, Salvucci GD, Entekhabi D (2018) Soil and atmospheric controls on the land surface energy balance: a generalized framework for distinguishing moisture-limited and energy-limited evaporation regimes. Water Resour Res 54(3):1831–1851. https://doi.org/10.1002/2017WR021729

Hirschi M, Stradiotti P, Crezee B, Dorigo W, Seneviratne SI (2025) Potential of long-term satellite observations and reanalysis products for characterising soil drying: trends and drought events. Hydrol Earth Syst Sci 29:397–425. https://doi.org/10.5194/hess-

Ho-Hagemann HTM, Hagemann S, Rockel B (2015) On the role of soil moisture in the generation of heavy rainfall during the Oder flood event in July 1997. Tellus A Dyn Meteorol Oceanogr. https://doi.org/10.3402/tellusa.v67.28661

Igbawua T, Zhang J, Yao F et al (2019) Assessment of moisture budget over West Africa using MERRA-2's aerological model and satellite data. Clim Dyn 52:83–106. https://doi.org/10.1007/s00382-018-4126-2

Jung M, Reichstein M, Ciais P, Seneviratne SI, Sheffield J, Goulden ML, Bonan G, Cescatti A, Chen J, De Jeu R, Dolman AJ, Eugster W, Gerten D, Gianelle D, Gobron N, Heinke J, Kimball J, Law BE, Montagnani L, Zhang K (2010) Recent decline in the global land evapotranspiration trend due to limited moisture supply. Nature 467(7318):951–954. https://doi.org/10.1038/nature09396

Kachi M, Naoki K, Hori M, Imaoka K (2013) AMSR2 validation results. In: 2013 IEEE international geoscience and remote sensing symposium-IGARSS (pp. 831–834). IEEE. https://doi.org/10.1109/IGARSS.2013.6721287

Kanniah KD, Beringer J, Hutley L (2013) Exploring the link between clouds, radiation, and canopy productivity of tropical savannas. Agric for Meteorol 182:304–313. https://doi.org/10.1016/j.agrformet.2013.06.010

Kenfack K, Tamoffo AT, Djiotang Tchotchou LA et al (2023) Assessment of uncertainties in reanalysis datasets in reproducing thermodynamic mechanisms in the moisture budget's provision in the Congo Basin. Theor Appl Climatol 154:613–626. https://doi.org/10.1007/s00704-023-04576-0

Kim Y, Park H, Kimball JS, Colliander A, McCabe MF (2023) Global estimates of daily evapotranspiration using SMAP surface and root-zone soil moisture. Remote Sens Environ 298:113803. https://doi.org/10.1016/j.rse.2023.113803

Koster RD, Dirmeyer PA, Guo Z, Bonan G, Chan E, Cox P, Gordon CT, Kanae S, Kowalczyk E, Lawrence D, Liu P, Lu CH, Malyshev S, McAvaney B, Mitchell K, Mocko D, Oki T, Oleson K, Pitman A, Sud YC, Taylor CM, Verseghy D, Vasic R, Xue Y, Yamada T, GLACE Team (2004) Regions of strong coupling between soil moisture and precipitation. Science 305(5687):1138–1140. https://doi.org/10.1126/science.1100217

Lion M, Kosugi Y, Takanashi S, Noguchi S, Itoh M, Katsuyama M, Matsuo N, Shamsuddin A (2017) Evapotranspiration and water source of a tropical rainforest in peninsular Malaysia. Hydrol Process 31(24):4338–4353. https://doi.org/10.1002/hyp.11360

Liu D, Wang G, Mei R, Yu Z, Gu H (2014) Diagnosing the strength of land-atmosphere coupling at subseasonal to seasonal time scales in Asia. J Hydrometeorol 15:320–339. https://doi.org/10.1175/JHM-D-13-0104.1

Liu X, Xu J, Zhou X, Wang W, Yang S (2020) Evaporative fraction and its application in estimating daily evapotranspiration of water-saving irrigated rice field. J Hydrol 584:124317. https://doi.org/10.1016/j.jhydrol.2019.124317

Lorenz R, Jaeger EB, Seneviratne SI (2010) Persistence of heat waves and its link to soil moisture memory. Geophys Res Lett. https://doi.org/10.1029/2010GL042764

Lorenz R, Pitman AJ, Hirsch AL, Srbinovsky J (2015) Intraseasonal versus interannual measures of land–atmosphere coupling strength in a global climate model: GLACE-1 versus GLACE-CMIP5 experiments in ACCESS1. 3b. J Hydrometeorol 16(5):2276–2295. https://doi.org/10.1175/JHM-D-14-0206.1

Lou W, Liu P, Cheng L, Li Z (2022) Identification of soil moisture–precipitation feedback based on temporal information partitioning networks. JAWRA J Am Water Resour Assoc 58(6):1199–1215. https://doi.org/10.1111/1752-1688.12978

Madhumali C, Wahala S, Sanjeewani N, Samarasinghe D, De Costa J (2024) Influence of climate, soil and vegetation diversity on the leaf area index as measured by canopy hemispherical photography in tropical rainforests across a wide elevational gradient. Geomatica 76(1):100001. https://doi.org/10.1016/j.geomat.2024.100001

McVicar TR, Roderick ML, Donohue RJ, Van Niel TG (2012) Less bluster ahead? Ecohydrological implications of global trends of terrestrial near-surface wind speeds. Ecohydrology 5(4):381–388. https://doi.org/10.1002/eco.1298

Miralles DG, De Jeu RAM, Gash JH, Holmes TRH, Dolman AJ (2011) Magnitude and variability of land evaporation and its components at the global scale. Hydrol Earth Syst Sci 15:967–981. https://doi.org/10.5194/hess-15-967-2011

Miralles DG, J. M, Gash JH, Parinussa RM, De Jeu RA, Beck HE, Holmes TR, Jiménez C, Verhoest NE, Dorigo WA, Teuling AJ, Johannes Dolman A (2014) El Niño–La Niña cycle and recent trends in continental evaporation. Nat Clim Chang 4(2):122–126. https://doi.org/10.1038/nclimate2068

Muñoz-Sabater J, Dutra E, Agustí-Panareda A, Albergel C, Arduini G, Balsamo G, Boussetta S, Choulga M, Harrigan S, Hersbach H, Martens B, Miralles DG, Piles M, Rodríguez-Fernández NJ, Zsoter E, Buontempo C, Thépaut JN (2021) ERA5-land: a state-of-the-art global reanalysis dataset for land applications. Earth Syst Sci Data 13(9):4349–4383. https://doi.org/10.5194/essd-13-4349-2021

Mwanthi AM, Mutemi JN, Dyer E, James R, Opijah FJ, Webb T, Artan G (2023) Representation of land–atmosphere coupling processes over Africa in coupled model intercomparison project Phase 6. Clim Dyn. https://doi.org/10.1007/s00382-023-06710-0

Nahayo L, Peng C, Lei Y et al (2023) Spatial understanding of historical and future landslide variation in Africa. Nat Hazards 119:613–641. https://doi.org/10.1007/s11069-023-06126-3

Nicholson SE, Funk C, Fink AH (2018) Rainfall over the African continent from the 19th through the 21st century. Glob Planet Change 165:114–127. https://doi.org/10.1016/j.gloplacha.2017.12.014

Nogueira M (2020) Inter-comparison of ERA-5, ERA-interim and GPCP rainfall over the last 40 years: process-based analysis of systematic and random differences. J Hydrol 583:124632

Peters T (2016) Water balance in tropical regions. In: Pancel L, Köhl M. (eds.) Tropical forestry handbook. Springer, Berlin, Heidelberg. https://doi.org/10.1007/978-3-642-54601-3_40

Pokam WM, Djiotang LAT, Mkankam FK (2012) Atmospheric water vapor transport and recycling in Equatorial Central Africa through NCEP/NCAR reanalysis data. Clim Dyn 38:1715–1729. https://doi.org/10.1007/s00382-011-1242-7

Power S, Delage F, Chung C, Kociuba G, Keay K (2013) Robust twenty-first-century projections of El Niño and related precipitation variability. Nature 502(7472):541–545. https://doi.org/10.1038/nature12580

Renée Brooks J, Barnard HR, Coulombe R, McDonnell JJ (2010) Ecohydrologic separation of water between trees and streams in a Mediterranean climate. Nat Geosci 3(2):100–104. https://doi.org/10.1038/ngeo722

Rousseeuw PJ (1987) Silhouettes: a graphical aid to the interpretation and validation of cluster analysis. J Comput Appl Math 20:53–65. https://doi.org/10.1016/0377-0427(87)90125-7

Santanello JA Jr., Peters-Lidard CD, Kumar SV (2011) Diagnosing the sensitivity of local land–atmosphere coupling via the soil moisture–boundary layer interaction. J Hydrometeorol 12:766–786. https://doi.org/10.1175/JHM-D-10-05014.1

Seneviratne SI, Lüthi D, Litschi M, Schär C (2006) Land–atmosphere coupling and climate change in Europe. Nature 443(7108):205–209. https://doi.org/10.1038/nature05095

Seneviratne SI, Corti T, Davin EL, Hirschi M, Jaeger EB, Lehner I, Orlowsky B, Teuling AJ (2010) Investigating soil moisture–climate interactions in a changing climate: a review. Earth-Sci Rev 99(3–4):125–161. https://doi.org/10.1016/j.earscirev.2010.02.004

Song X, Leng P, Li X, Li X, Ma J (2012) Retrieval of daily evolution of soil moisture from satellite-derived land surface temperature and net surface shortwave radiation. Int J Remote Sens 34(9–10):3289–3298. https://doi.org/10.1080/01431161.2012.716915

Song H, Braeckevelt E, Zhang P, Sha Q, Zhou J, Liu T, Wu S, Lu Y, Klemm O (2017) Evapotranspiration from a primary subtropical evergreen forest in Southwest China. Ecohydrol 10(4):e1826. https://doi.org/10.1002/eco.1826

Sun S, Wang G (2012) The complexity of using a feedback parameter to quantify the soil moisture-precipitation relationship. J Geophys Res Atmos. https://doi.org/10.1029/2011JD017173

Teuling AJ, Hirschi M, Ohmura A, Wild M, Reichstein M, Ciais P, Buchmann N, Ammann C, Montagnani L, Richardson AD, Wohlfahrt G, Seneviratne SI (2009) A regional perspective on trends in continental evaporation. Geophys Res Lett 36:L02404. https://doi.org/10.1029/2008GL036584

Thorndike RL (1953) Who belongs in the family? Psychometrika 18:267–276. https://doi.org/10.1007/BF02289263

Vidale PL, Lüthi D, Wegmann R et al (2007) European summer climate variability in a heterogeneous multi-model ensemble. Clim Change 81(Suppl 1):209–232. https://doi.org/10.1007/s10584-006-9218-z

Washington R, James R, Pearce H, Pokam WM, Moufouma-Okia W (2013) Congo Basin rainfall climatology: can we believe the climate models? Philos Trans R Soc Lond B Biol Sci 368(1625):20120296. https://doi.org/10.1098/rstb.2012.0296

Wei J, Dirmeyer PA (2010) Toward understanding the large-scale land-atmosphere coupling in the models: roles of different processes. Geophys Res Lett. https://doi.org/10.1029/2010GL044769

Wild M, Grieser J, Schär C (2008) Combined surface solar brightening and increasing greenhouse effect support recent intensification of the global land-based hydrological cycle. Geophys Res Lett. https://doi.org/10.1029/2008GL034842

Wilks DS (2011) Statistical methods in the atmospheric sciences (Vol. 100). Academic press

Worden S, Fu R, Chakraborty S, Liu J, Worden J (2021) Where does moisture come from over the Congo Basin? J Geophys Res Biogeosci 126(8):e2020JG006024. https://doi.org/10.1029/2020JG006024

Worden S, Bloom AA, Worden J, Levine P, Shi M, Fu R (2024) Congo Basin water balance and terrestrial fluxes inferred from satellite observations of the isotopic composition of water vapor. Water Resour Res 60(7):e2023WR035092. https://doi.org/10.1029/2023WR035092

Wu H, Xu X, Luo T, Yang Y, Xiong Z, Wang Y (2022) Variation and comparison of cloud cover in MODIS and four reanalysis datasets of ERA-interim, ERA5, MERRA-2 and NCEP. Atmos Res 281:106477. https://doi.org/10.1016/j.atmosres.2022.106477

Xing Z, Fan L, Zhao L, De Lannoy G, Frappart F, Peng J, Wigneron JP (2021) A first assessment of satellite and reanalysis estimates of surface and root-zone soil moisture over the permafrost region of Qinghai-Tibet Plateau. Remote Sens Environ 265:112666. https://doi.org/10.1016/j.rse.2021.112666

Yao P, Lu H, Shi J et al (2021) A long term global daily soil moisture dataset derived from AMSR-E and AMSR2 (2002–2019). Sci Data 8:143. https://doi.org/10.1038/s41597-021-00925-8

Zhang L, Dawes WR, Walker GR (2001) Response of mean annual evapotranspiration to vegetation changes at catchment scale. Water Resour Res 37(3):701–708. https://doi.org/10.1029/2000WR900325

Zhang J, Wang W-C, Wei J (2008) Assessing land-atmosphere coupling using soil moisture from the Global Land Data Assimilation System and observational precipitation. J Geophys Res 113:D17119. https://doi.org/10.1029/2008JD009807

Zhang K, Kimball JS, Nemani RR, Running SW, Hong Y, Gourley JJ, Yu ZB (2015) Vegetation greening and climate change promote multi decadal rises of global land evapotranspiration. Sci Rep 5:15956. https://doi.org/10.1038/srep15956

Zhang Y, Chiew S, F. H., Peña-Arancibia J, Sun F, Li H, Leuning R (2017) Global variation of transpiration and soil evaporation and the role of their major climate drivers. J Geophys Res Atmos 122(13):6868–6881. https://doi.org/10.1002/2017JD027025

Zhang T, Shen S, Cheng C et al (2018) Long-range correlation analysis of soil temperature and moisture on A'rou hillsides, Babao River Basin. J Geophys Res Atmos 123:12606–12620. https://doi.org/10.1029/2018JD029094

Zhou L, Tian Y, Myneni RB, Ciais P, Saatchi S, Liu YY, Piao S, Chen H, Vermote EF, Song C, Hwang T (2014) Widespread decline of Congo rainforest greenness in the past decade. Nature 509(7498):86–90. https://doi.org/10.1038/nature13265

Nicholson SE (2018) The ITCZ and the Seasonal Cycle over Equatorial Africa. Bull Amer Meteor Soc 99:337–348. https://doi.org/10.1175/BAMS-D-16-0287.1

Quesada B, Vautard R, Yiou P, Hirschi M, Seneviratne SI (2012) Asymmetric European summer heat predictability from wet and dry southern winters and springs. Nat Clim Change 2(10):736–741. https://doi.org/10.1038/nclimate1536

Varian H (2005) Bootstrap tutorial. Mathematica J 9(4):768–775

Peng J, Albergel C, Balenzano A, Brocca L, Cartus O, Cosh MH, Crow WT, Dabrowska-Zielinska K, Dadson S, Davidson MW, De Rosnay P, Dorigo W, Gruber A, Hagemann S, Hirschi M, Kerr YH, Lovergine F, Mahecha MD, Marzahn P, Loew A (2020) A roadmap for high-resolution satellite soil moisture applications – confronting product characteristics with user requirements. Remote Sens Environ 252:112162. https://doi.org/10.1016/j.rse.2020.112162

Srivastava PK, Han D, Rico-Ramirez MA et al (2013) Data Fusion Techniques for Improving Soil Moisture Deficit Using SMOS Satellite and WRF-NOAH Land Surface Model. Water Resour Manage 27:5069–5087. https://doi.org/10.1007/s11269-013-0452-7

Sadri S, Pan M, Wada Y, Vergopolan N, Sheffield J, Famiglietti JS, Kerr Y, Wood E (2020) A global near-real-time soil moisture index monitor for food security using integrated SMOS and SMAP. Remote Sens Environ 246:111864. https://doi.org/10.1016/j.rse.2020.111864

Jaksa WT, Sridhar V (2015) Effect of irrigation in simulating long-term evapotranspiration climatology in a human-dominated river

basin system. Agric For Meteorol 200:109–118. https://doi.org/10.1016/j.agrformet.2014.09.008

Sridhar V, Hubbard KG, You J, Hunt ED (2008) Development of the Soil Moisture Index to Quantify Agricultural Drought and Its User Friendliness in Severity-Area-Duration Assessment. J Hydrometeor 9:660–676. https://doi.org/10.1175/2007JHM892.1